Incoming Exchange Student - Master Thesis

Erasmus □ Techno □ Other (specify):

Title of master course:

Title of master thesis: Prediction of low-cycle fatigue in a cantilever bending element: experimental tests and model prediction

Document: Master Thesis

Student (Name & Surname)**:** Tim Goemaere

EPS Advisor: Xavier Cahis
Department: Eng. Mecànica i de la Construcció Industrial

Delivered on(month/year):June/2015

Table of contents

1 Introduction

1.1 Abstract

TADAS-devices are used in special moment resisting frames and needs certain relative displacements to start energy dissipating. The TADAS (triangular-plate added damping and stiffness) device is one of the examples of hysteretic dampers with elasto-plastic behavior. A TADAS-device is designed and tested on low-cycle fatigue. A test design from a preliminary test is proposed.

1.2 Objective

The objective is to design a TADAS-device ant the testing set-up. The design is improved, taking into account the knowledge gained during the process.

1.3 Methodology

First a TADAS-device is designed so that every part of the device yields at the same time for a given displacement. Then the testing set-up is designed and improved several times. Afterwards some tests are done and new problems are discovered. At the end the conclusions are made in view of a future design.

1.4 Contents

After the introduction this work has different chapters, a small summary is given:

- State of the art:

  There is some information given about the use of hysteretic dampers, TADAS hysteretic dampers and low-cycle fatigue.

- Design:

  The yielding displacement is determined. With this yielding displacement the geometry of TADAS-device is searched, taking into account the yielding length and the width. With the geometry the theoretical force is calculated and a proposal of design is made. There is also an estimate of the cost made and the dimensions of the tensile specimen are determined.

- Set-up:

  Several testing set-ups are designed and the final geometry of the TADAS-specimen is given. There is also a control made for the tensile strength of the bolt on the left part of the device which will be clamped. In Annex B the geometry of the pieces that have to be made for the testing set-up is included.

- TADAS-specimen in *ANSYS Workbench*

  The TADAS-specimen is simplified and made in *ANSYS Workbench* to have an idea about the real deformation under a given force. A mesh is made, the boundary conditions are determined and a remote force is applied. The directional deformation and the equivalent (von-Mises) stress are computed.

- Testing method:

  Different loading protocols for the tests are explained, together with the software which will control the piston of the machine.

- Tests:

  A diagram is given about how the tests will take place. The several transducers are indicated with some information about them. The different tests are explained and some conclusions are made.

- Proposal of future design:

  A new proposal for future design is made, taking into account the knowledge gained during the tests.

- Conclusion:

  The conclusions about the TADAS-device and the testing set-up are made based on the knowledge gained from the tests.

- Acknowledgement:

  The people who assisted me and made it possible to make this master thesis are thanked.

- Bibliography

  A summary about the used references is given.

- Annexes

  Some annexes are included to this master thesis:

  - Annex A: Glossary of symbols
  - Annex B: Geometry of the pieces of the testing set-up
  - Annex C: Technical specifications of load cell MODELO 630

2 State of the art

2.1 Use of hysteretic dampers

There exist various damping mechanisms intended to provide positive control of structural vibration induced by earthquakes, one of them are the hysteretic dampers. They dissipate the energy exerted into the structure making use of their hysteresis (Inoue & Kuwahara, 1998). The hysteretic damper is also one of the most widely used energy dissipating devices due to its good balance between cost and efficiency. A disadvantage is the fact that evaluating the health of the hysteretic damper after a seismic event is a matter of great concern. This is because both yield and phase transformation of metals involve inelastic strains in the material which can be considered as damage (Gallego, Benavent-Climent, & Romo-Melo, 2015).

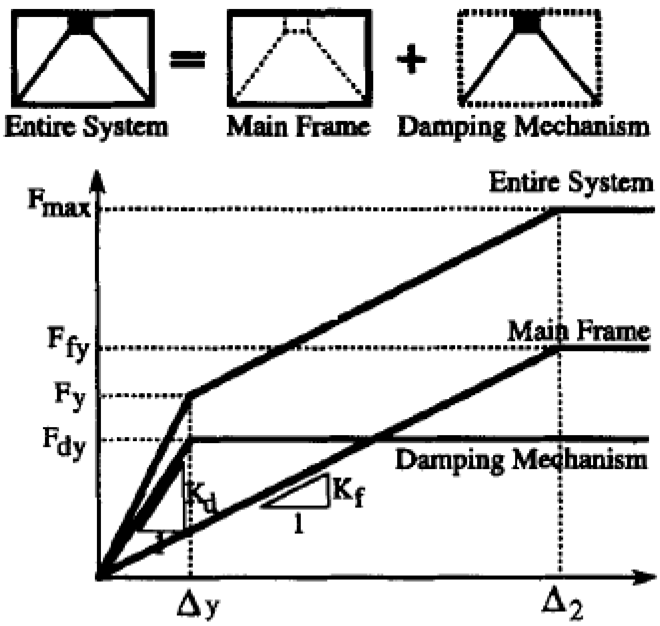

Figure1: Schematic hysteretic behavior of structures with hysteretic dampers (Nakashima, Saburi, & Tsuji, 1996)

The resistance behavior of a structural system with a hysteretic damper can be simplified as shown in Figure 1. The system consists of a main frame (serving primarily as the gravity force carrying system) and a hysteretic damping mechanism, with the two components linked in parallel (Nakashima, Saburi, & Tsuji, 1996). An example of hysteretic dampers in building are BRB's (Buckling Restrained Braces). The dampers are mostly installed on every storey as shown in Figure 2 (Open Steel Joists).

Figure 2: Section of buckling restrained brace (Open Steel Joists)

2.2 TADAS hysteretic dampers

Added Damping and Stiffness devices are popular metallic energy dissipation devices. These devices can sustain a large amount of earthquake input energy with a good predictable performance. They need a certain relative displacement to start energy dissipating and have their best performance in a severe earthquake where they can dissipate a very reliable large amount of energy. Triangular-plate Added Damping and Stiffness devices concentrates energy dissipation at locations that have been designed for this purpose, so it substantially reduces the energy dissipation demand on other structural members. The yielding of the device will not affect the gravity load service capacity of the structural system, because the devices are only part of the lateral load resisting system. They can easily be replaced after an earthquake if necessary (Dareini & Hashemi, 2011).The amount of energy the system can dissipate depends on the geometry of the TADAS-device and the number of TADAS-devices integrated in the system. The reason that TADAS-devices and not ADAS-devices are chosen, is because they are easier to test.

2.3 Low-cycle fatigue

Fatigue is a phenomenon that occurs when the device is subjected to cyclic loading. Because of the repeatedly applied loads, the material loses a piece of his strength. Fatigue is also one of the primary reasons for the failure of structural components. The life of a fatigue crack has two parts: initiation and propagation (Ganesh, et al., 2014). The initiation of micro-cracks is due to local accumulation of dislocations, high stresses at local points, plastic deformation around inhomogeneous inclusions or other imperfections in or under the contact surface. After the crack is occurred, it propagates which causes permanent damage to a mechanical element (Fajdiga & Sraml, 2009).

Low-cycle fatigue is characterized by large inelastic amplitudes (several times the yield strength) and a rather small number of cycles to failure, which is usually less than 10^2 cycles (Zhou, Wang, Yang, & Shi, 2014).

3 Design

First the yielding displacement is determined. With this yielding displacement there is searched for a geometry of the TADAS-device taking into account the yielding length and the width. Also the theoretical yielding force is calculated. A proposal of design is made together with an estimate of the cost. Also the dimensions of the tensile specimen are determined.

3.1 Yielding displacement Δ_y

Moment resisting frames is a method used to resist lateral loads, especially during an earthquake (Mahmoudi & Abdi, 2011). The design displacement corresponding to the interstory drift has been considered as 1% of the story height (Piedrafita, Cahis, Simon, & Comas, 2015). If the story height is considered equal to 3 m, then the design displacement becomes 30 mm. From this design displacement and considering a ductility of 5 - where the ductility is the ration of the design displacement and the yielding displacement - a yielding displacement of 6 mm is obtained.

3.2 Geometry and deformation

3.2.1 Yielding length

First the yielding length is found by trial and error. The characteristics of the steel are considered as:

- Young's modulus: 200 000 MPa
- Yielding stress: 235 MPa

Remark: A glossary of symbols is added in Annex A.

<u>Length = 160 mm</u>

Strain:

$$\varepsilon_y = \frac{\sigma_y}{E} = \frac{235}{2 * 10^5} = 0{,}001175$$

Where ε_y is the yielding strain, σ_y is the yielding stress and E is the Young's modulus.

Radius of curvature:

$$\varepsilon_y = \frac{y_{max}}{\rho} = \frac{\frac{t}{2}}{\rho} \rightarrow \rho = \frac{\frac{t}{2}}{\varepsilon_y} = \frac{\frac{5}{2}}{0{,}001175} = 2127{,}66\ mm$$

Where y_{max} is the distance from the centroidal axis to the end of the section, ρ is the radius of curvature and t is the thickness of the specimen.

Angle:

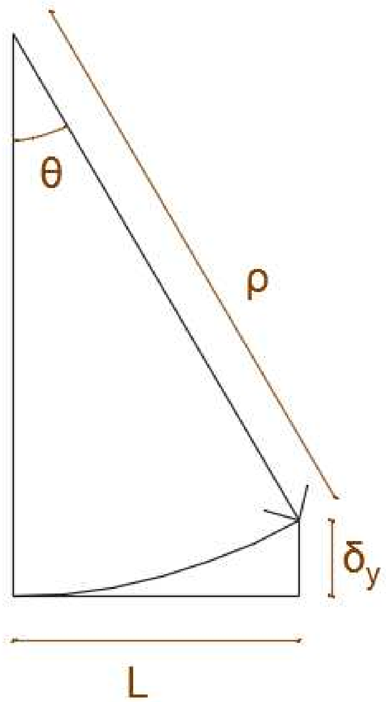

Figure 3: Radius of curvature

$$\theta = \frac{L}{\rho} = \frac{160}{2127{,}66} = 0{,}0752\ rad$$

Where θ is the angle and L is the length of the specimen.

Displacement:

- $\Delta_{\mathrm{y}} = \delta_y = \rho * (1 - \cos(\theta)) = 2127{,}66 * (1 - \cos(0{,}0752)) = 6{,}01\ mm$
- $\Delta_{\mathrm{D}} = 5 * \delta_y = 30{,}07\ mm$

Where Δ_{y} is the yielding displacement and Δ_{D} is the design displacement.

This value of the yielding displacement Δ_{y} is very close to the wanted value. A yielding length of 160 mm is used.

3.2.2 Width

The width of the device is calculated taking into account the radius of curvature should be the same in each point of the section. In this case every part of the device yields at the same time.

Calculation of B_2:

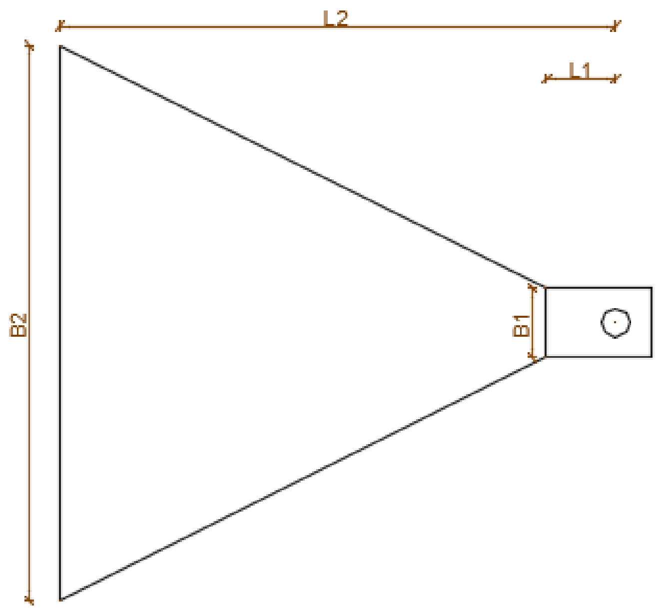

Figure 4: Calculation of B2

$$\frac{1}{\rho} = \frac{M}{E * I} = cte$$

Where M is the bending moment and I is the moment of inertia.

$$\frac{M_1}{E * I_1} = \frac{M_2}{E * I_2} \to \frac{M_1}{I_1} = \frac{M_2}{I_2}$$

- $M_1 = F * L_1$
- $M_2 = F * L_2$

Where F is the force applied on the specimen, L_1 and L_2 are indicated on Figure 4: Calculation of B2Figure 4.

$$\frac{L_1}{L_2} = \frac{I_1}{I_2} = \frac{\frac{B_1 * t^3}{12}}{\frac{B_2 * th^3}{12}} = \frac{B_1}{B_2}$$

$$\to B_2 = B_1 * \frac{L_2}{L_1}$$

Where B_1 and B_2 are indicated on Figure 4.

A choice is made for the other dimension and from this the length of B_2 is obtained:

- $B_1 = 20\ mm$
- $L_1 = 20\ mm$
- $L_2 = 160\ mm$

$\rightarrow B_2 = 160\ mm$

3.2.3 Theoretical yielding force

The applied force is calculated to obtain the same stresses in every part of the device.

$$\frac{1}{\rho} = \frac{M_2}{E * I_2} \rightarrow M_2 = \frac{E * \frac{B_2 * t^3}{12}}{\rho} = \frac{2 * 10^5 * \frac{160 * 5^3}{12}}{2127{,}66} = 156\ 667\ Nmm$$

$$F = \frac{M_2}{L_2} = 979{,}17\ N$$

3.3 Proposal of design

The design is made taking into account the dimensions chosen and calculated in the previous steps. At the right and at the left there is added a part to the device that will be clamped:

- At the left there is added a part to the device with a length of 60 mm which will be clamped. The width goes to 170 mm because it's not advisable to have a corner in a part that's subjected to forces and deformations. If this were the case, there would be a high stress concentration in the corner.
- At the right there is added a part to the device of 10 mm which also will be clamped, so the yielding length of 160 mm is still obtained.

Where the width of the device goes to 20 mm, there would also be a stress concentration in the corner. To reduce this stress concentration a fillet with a radius of 15 mm is chosen.

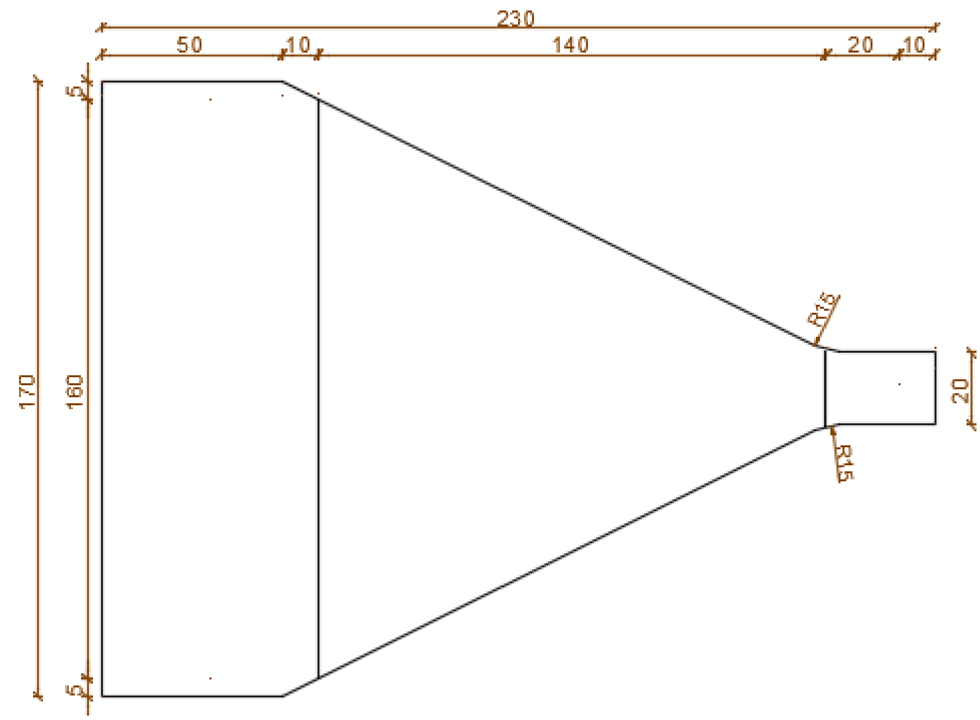

Figure 5: First design TADAS-specimen

3.4 Tensile specimen

Tensile specimens have to be provided from the same piece of metal where the dissipators will be obtained from. Its longitudinal axis has to be oriented in the same way as the longitudinal axis of the TADAS-specimens manufactured out of this piece of metal. The tensile specimens will be tested following EN 10002-1 (European Committee for Standardization (CEN), 2001). A maximum ratio of 8 has to be guaranteed between the width and the thickness of the tensile specimen.

The chosen dimensions are:

- Width = 30 mm
- Thickness = 5 mm

Original gauge length:

$$L_0 = k * \sqrt{S_0} = 5{,}65 * \sqrt{30 * 5} = 69{,}2\, mm$$

Where L_0 is the original gauge length, k is the coefficient of proportionality and S_0 is the original cross-sectional area of the parallel length.

Minimum parallel length of machined test piece:

$$L_c = L_0 + 1{,}5 * \sqrt{S_0} = 69{,}2 + 1{,}5 * \sqrt{30 * 5} = 87{,}6\ mm$$

Where L_c is the parallel length.

The minimum length of the tensile specimen has to be 87,6 mm but this specimen has also to be clamped in at both ends. The total length is taken as 300 mm.

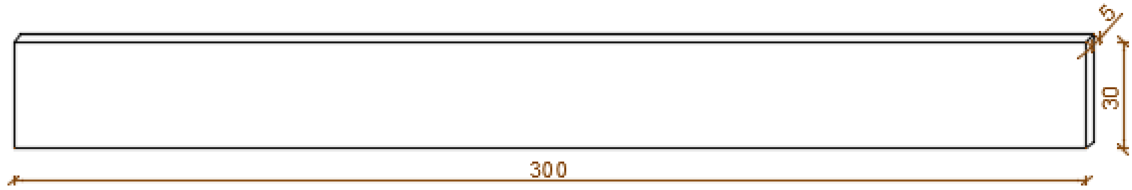

Figure 6: Design tensile specimen

3.5 Weight

The weight is calculated in order to have a thought of the cost price. The material cost of steel cut by laser is approximately €2/kg.

TADAS-specimen:

- $Area = 23\,429\ mm^2$ (Calculated by Autodesk AutoCAD 2015 – STUDENT VERSION)
- $Volume = 23\,429 * 5 = 117\,145\ mm^3$
- $Weight = 7900\ \frac{kg}{m^3} * 10^{-9} * 117\,145 = 0{,}925\ kg$

Tensile specimen:

- $Volume = 300 * 30 * 5 = 45\,000\ mm^2$
- $Weight = 7900\ \frac{kg}{m^3} * 10^{-9} * 45\,000 = 0{,}356\ kg$

4 Set-up

The tests are made in the Structural Laboratory of the AMADE research group at the University of Girona (Spain). In this Structural Laboratory there are 2 machines tooled with a piston which can be used to perform the tests.

4.1 Design option 1

The TADAS device would be tested with this machine. The piston has a load range of 30 tons of compression to 30 tons of extraction. The software used to control the piston is *PCD 2K*. The software is from Servosis S.L. (Servosis S.L.)

Figure 7: Machine 1

Figure 8: Ending of the piston, provided with a load cell of 300 kN of capacity

There is a hole ∅30 mm in the piston and a load cell MODELO 630 is available with a nominal load of 2500 kg (technical specifications in Annex C). All the other pieces of the set-up had to be designed and made. All the drawings are made in *Autodesk AutoCAD 2015 – STUDENT VERSION*.

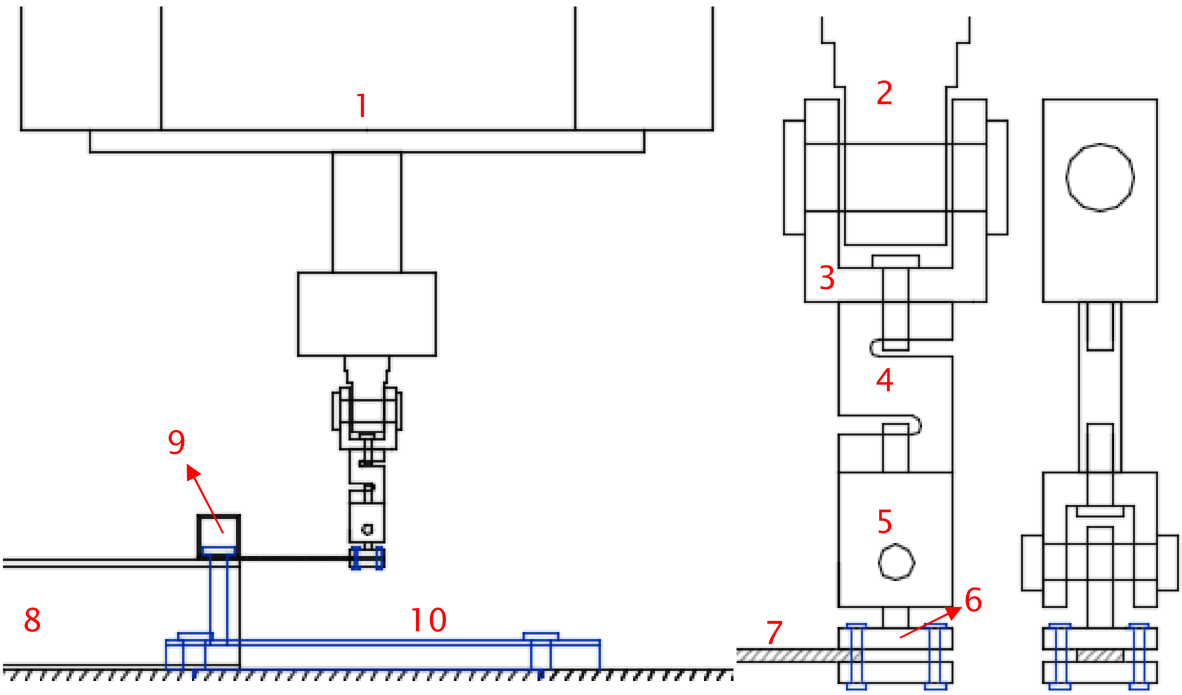

Figure 9: Design option 1

Explanation of the numbers on Figure 9:

1. Fixed frame of the machine
2. Piston of the machine, provided with a load cell of 30 tons of capacity
3. Design piece 1
4. Load cell MODELO 630, nominal load of 2500 kg.
5. Design piece 2
6. Design piece 3
7. TADAS-specimen
8. I-profile
9. Design piece 4
10. Design piece 5

There had to be designed a system to provide free rotation to the TADAS-specimen in the non-clamped ending. For this reason a rotation system was designed between the load cell and the specimen. All the pieces were designed but it was very complicated to clamp the left part of the specimen. In this design the TADAS-specimen lies on a I-profile (8) with a beam (9) on top of it. This beam had to be attached into the ground. On the ground there are holes where a beam (10) can be attached every 500 mm in a square shape.

Figure 10: Bolted holes in the ground

There were holes needed in the beam (9) located on top of the specimen (7) for bolts that had to be bolted into beams on the ground (10). Then these beams should have been fixed with bolts bolted into the holes in the ground. The numbers of Figure 11 refer to the same numbers used in Figure 9.

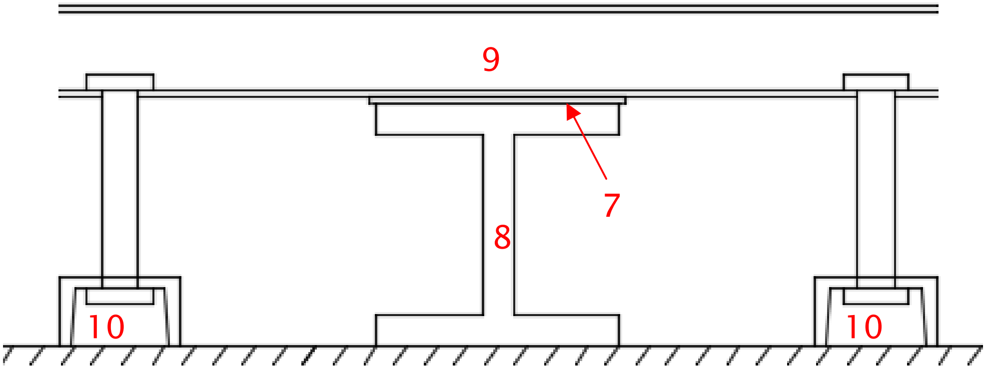

Figure 11: Cross-section left part of design option 1

For this set-up there had to be a lot of pieces made to be able to test the TADAS-specimen. It was advisable to search for a new design option.

4.2 Design option 2

The TADAS-device would be tested with another machine. The piston has a load range of 60 tons of compression to 60 tons of extraction. The software used for the measurements is *PCD 2K* (Servosis S.L.).

Figure 12: Machine 2

The design was also made in *Autodesk AutoCAD 2015 – STUDENT VERSION.*

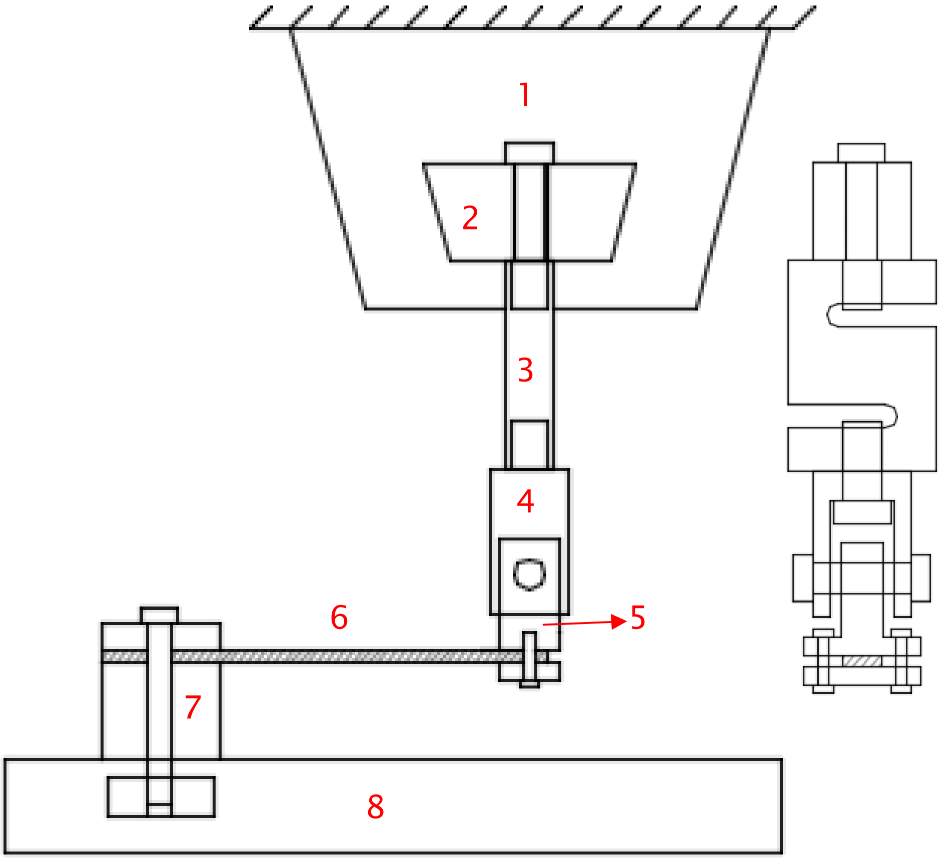

Figure 13: Design option 2

Explanation of the numbers on Figure 13:

1. Fixed frame of the machine
2. Available piece
3. Load cell MODELO 630, nominal load of 2500 kg.
4. Design piece 1
5. Design piece 2
6. TADAS-specimen
7. Design piece 3
8. Mobile head of the machine

The top piece of the set-up was already available in the lab and the method to clamp the left part of the specimen was much easier, so there were less pieces needed to be made. The system works in the same way as in design option 1. In this design the left part of the device was clamped using a bolt.

The bolt is screwed in a piece that's located in the slot of the mobile head of the machine. The right part was clamped in using 2 plates of steel, connected with a bolt on each side of the specimen.

4.3 Design option 3

The lowest part of the set-up could be simplified and the block under the left part of the specimen needed to be taller to allow all the deformations of the specimen during the tests.

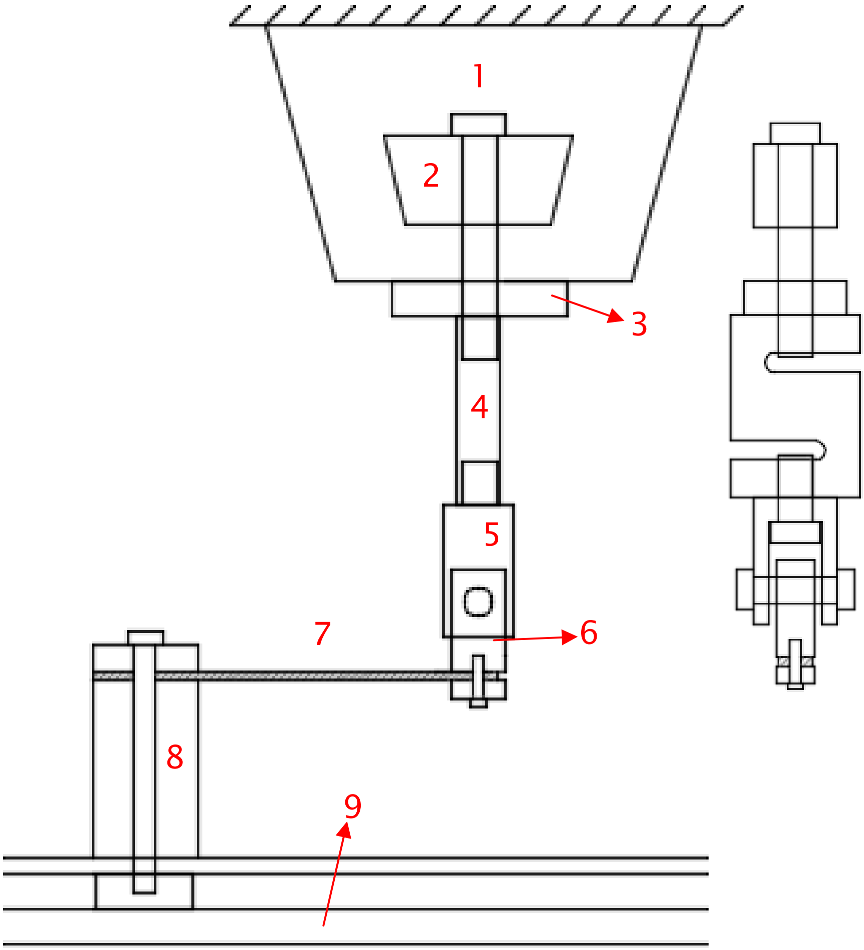

Figure 14: Design option 3

Explanation of the numbers on Figure 13:

1. Fixed frame of the machine
2. Available piece
3. Design piece 1
4. Load cell MODELO 630, nominal load of 2500 kg.

5. Design piece 2
6. Design piece 3
7. TADAS-specimen
8. Design piece 4
9. Mobile head of the machine

At the upper right part there had to be added a stiff plate so design piece 1 can keep its position when the piston is moving upwards.

Figure 15: Top of machine 2

Because the TADAS-specimen is bolted at the left and at the right, the design of the device had to be changed.

4.3.1 Final geometry of the TADAS-specimen

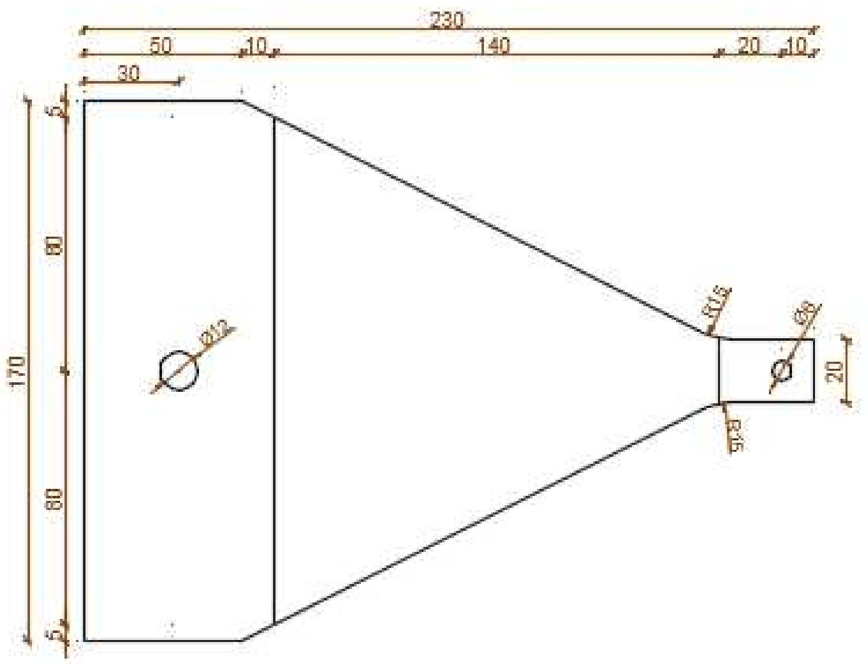

Figure 16: Final geometry TADAS-specimen

For the left part there is chosen for a bolt connection M12 8.8 ISO. It has to be checked if the bolt can withstand the forces.

4.3.2 Control tensile strength bolt

<u>Required tensile strength:</u>

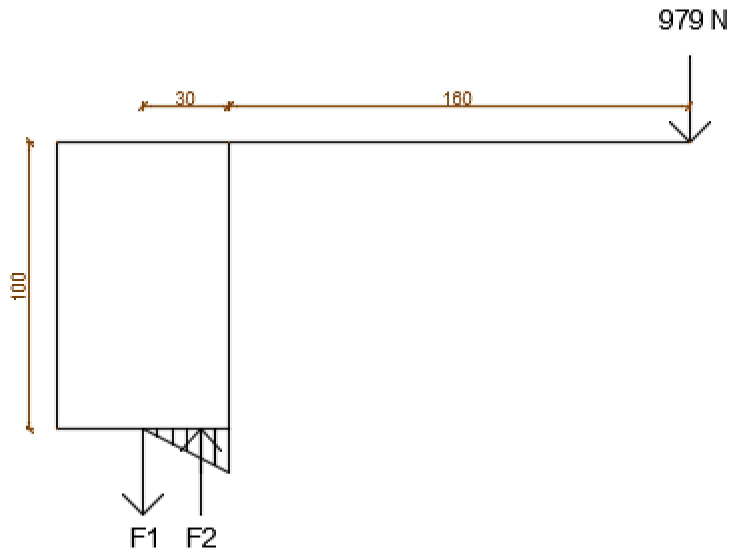

Figure 17: Sketch of the calculation of the required tensile strength

The calculation is simplified to have an idea if the bolt can withstand the forces.

- $\Sigma F_v = 0$
    - $F_1 - F_2 + 979 = 0$
    - $F_1 = F_b$
    - $F_2 = \frac{\sigma * b * x}{2}$

$$\rightarrow F_b - \frac{\sigma * b * x}{2} + 979 = 0$$

F_1 and F_2 are indicated on Figure 17, F_b is the required tensile strength of the bolt σ is the pressure on the triangular shaped zone on Figure 17, b is the width of design piece 4 and x is the length of the base of the triangular shaped zone.

- $\Sigma M_1 = 0$
    - $\frac{\sigma * b * x}{2}\left(x - \frac{1}{3}x\right) = 979 * 190$

$$\rightarrow \frac{\sigma * b * x}{2} = \frac{979 * 190}{x - \frac{1}{3}x}$$

For x the value of 30 mm is chosen:

- $F_b = \frac{979*190}{30-\frac{1}{3}*30} - 979 = 8322\ N$

<u>Maximum tensile strength:</u>

These calculation is made with NBN EN 1993-1-8 AC2009 (Bureau voor Normalisatie, 2005).

M12

- $A_s\ =\ 84{,}3\ mm^2$

8.8 ISO

- $f_{ub} = 800\ Mpa$
- $f_{yb} = 640\ Mpa$

Where A_s is the stress section of the bolt, f_{ub} is the ultimate tensile strength of the bolt and f_{yb} is the yielding tensile strength of the bolt.

Tensile strength:

$$F_{t,Rd} = \frac{k_2 * f_{ub} * A_s}{\gamma_{M2}}$$

$$F_{t,Rd} = \frac{0{,}9 * 800 * 84{,}3}{1{,}25} = 48\,557\ N$$

Where $F_{t,Rd}$ is the design value of the tensile strength per bolt.

Conclusion:

$$F_b \ll F_{t,Rd}$$
$$8322\ N \ll 48557\ N$$

The calculation does not have to be made more in detail because there is a big difference between the designed tensile strength and the maximum tensile strength. The chosen bolt connection M12 8.8 ISO complies.

4.3.3 Geometry of the pieces

The geometry of the available piece, the Load cell MODELO 630 and the 5 design pieces is given in Annex B. The technical information of the load cell is given in Annex C.

5 TADAS-specimen in *ANSYS Workbench*

The deformation in reality is not the same as the theoretical calculated deformation because the conditions can't be optimal. The software ANSYS *Workbench* is used to calculate the real deformation.

5.1 Geometry

The TADAS-specimen is simplified in *ANSYS Workbench*. The left part of the specimen that will be clamped is not taken into account in this model. It's assumed that the results of the simplification will approach the testing results.

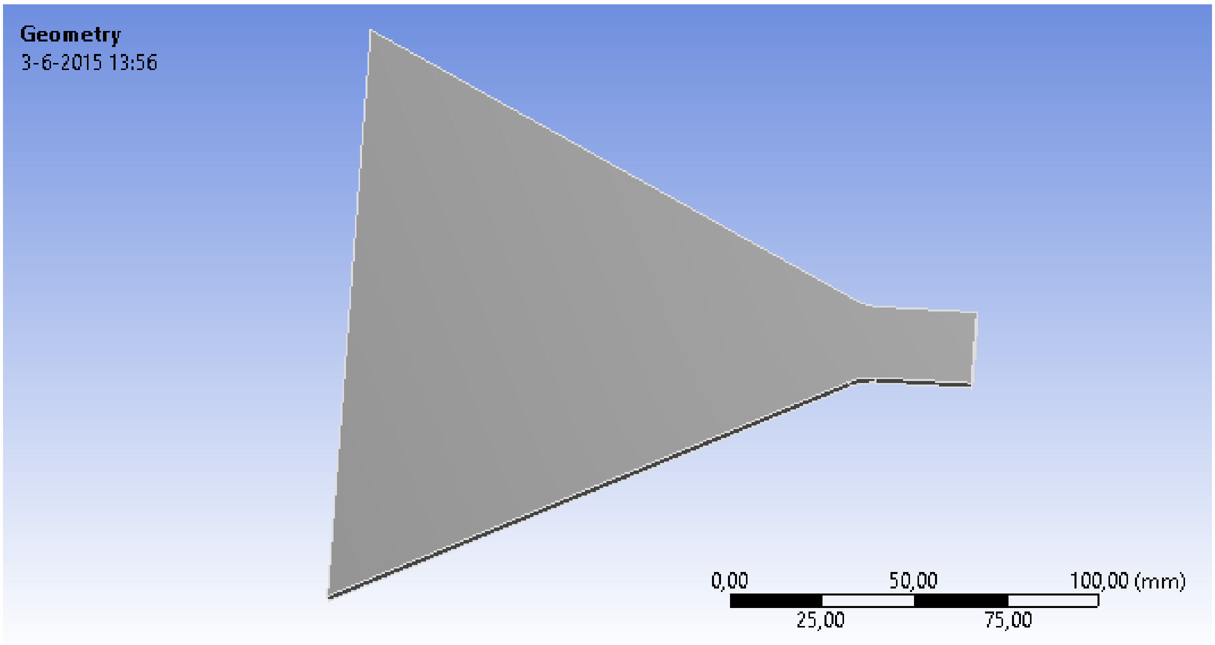

Figure 18: *ANSYS Workbench*: geometry

5.2 Mesh

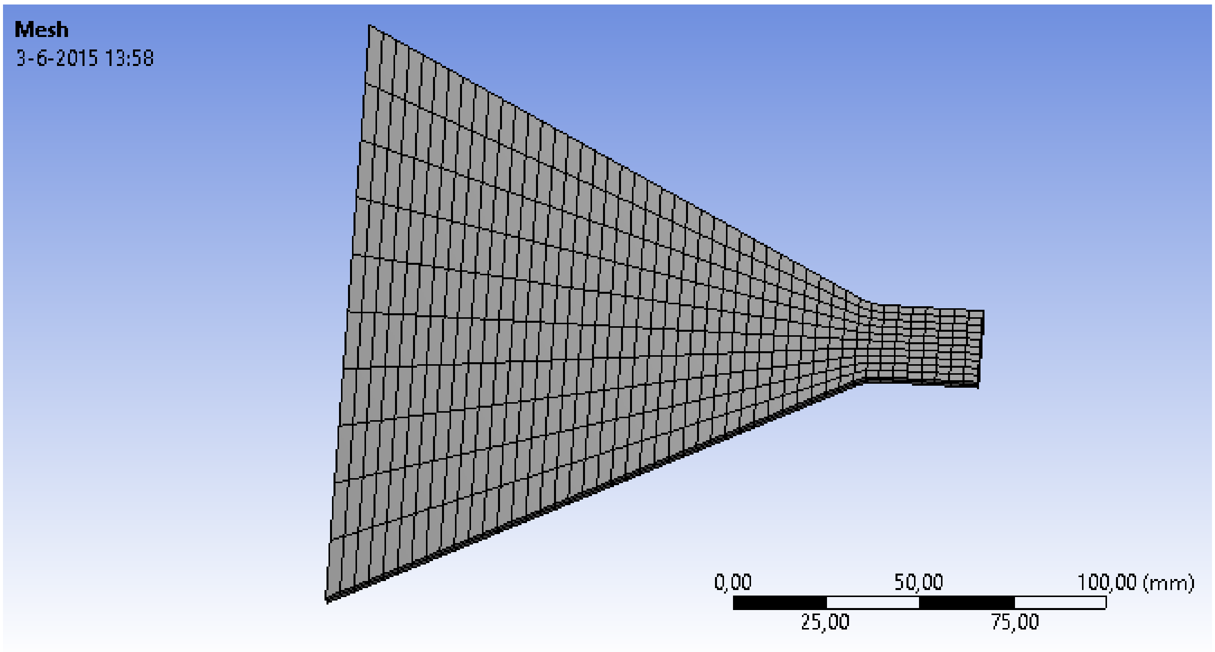

Figure 19: *ANSYS Workbench*: mesh

5.3 Fixed support

The left face of the device is fixed.

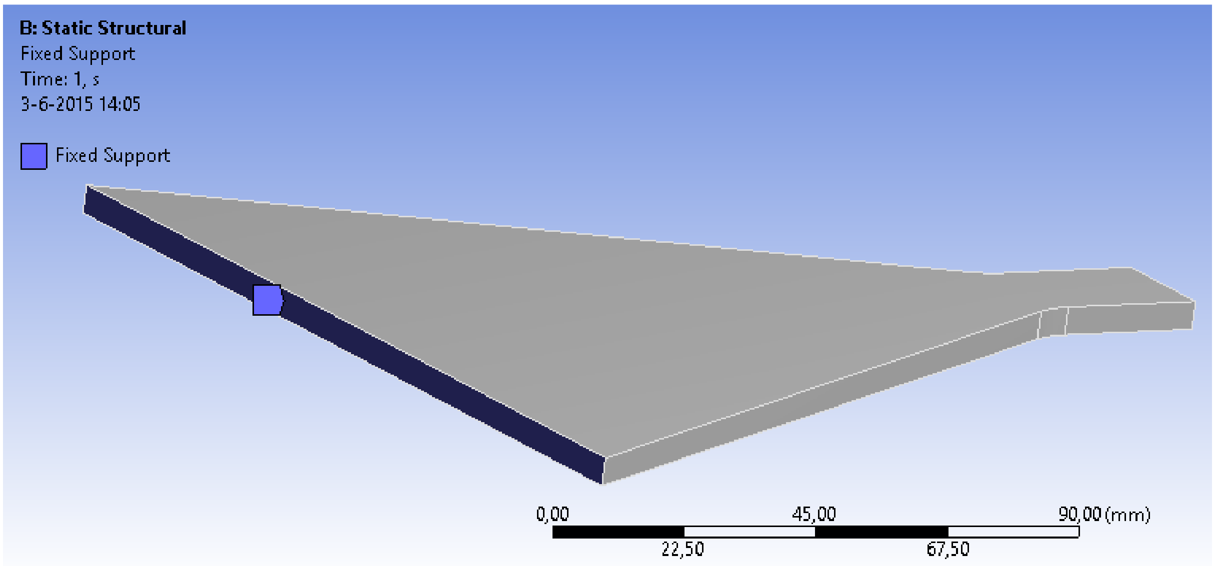

Figure 20: *ANSYS Workbench*: fixed support

5.4 Remote force

A remote force is used because remote boundary conditions provide the capability to capture the effect of a condition whose center of action is not directly located on the model without modelling details of the feature. The remote force applied is 979 N as calculated theoretically (ANSYS, 2015).

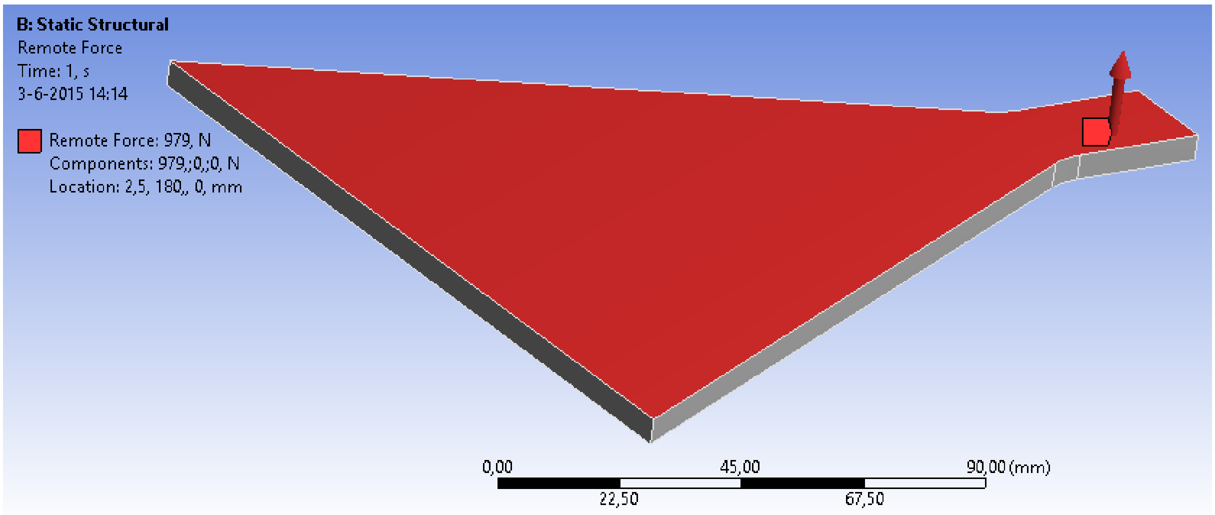

Figure 21: *ANSYS Workbench*: remote force

5.5 Directional deformation

The directional deformation in x-direction is 5,15 mm. This value is close to the theoretically calculated value of 6,01 mm.

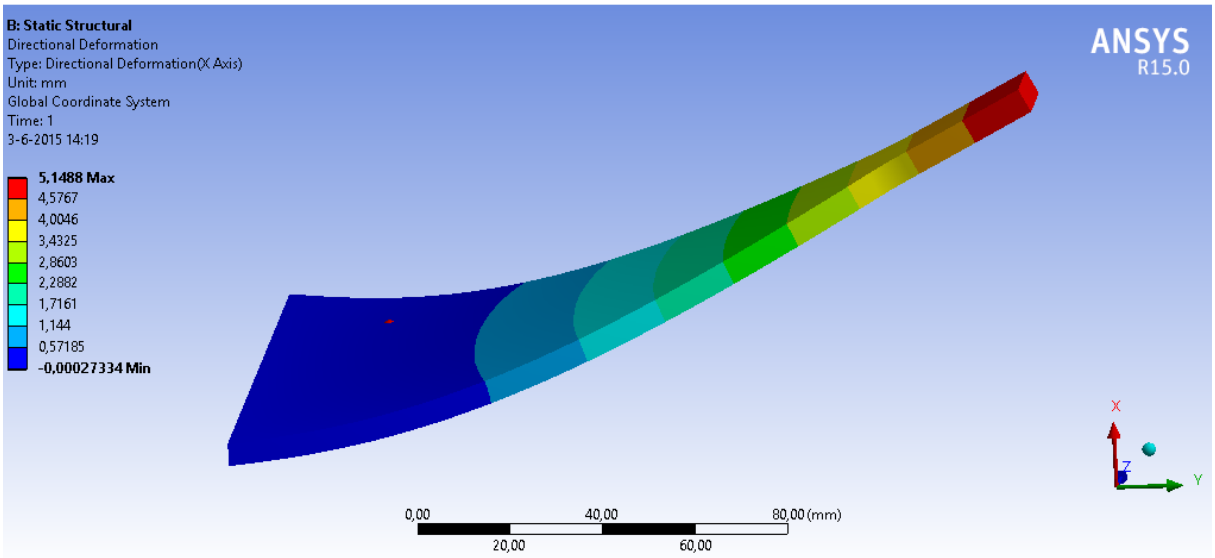

Figure 22: ANSYS Workbench: directional deformation

5.6 Equivalent (von-Mises) stress

The maximum equivalent (von-Mises) stress is 285,65 Mpa.

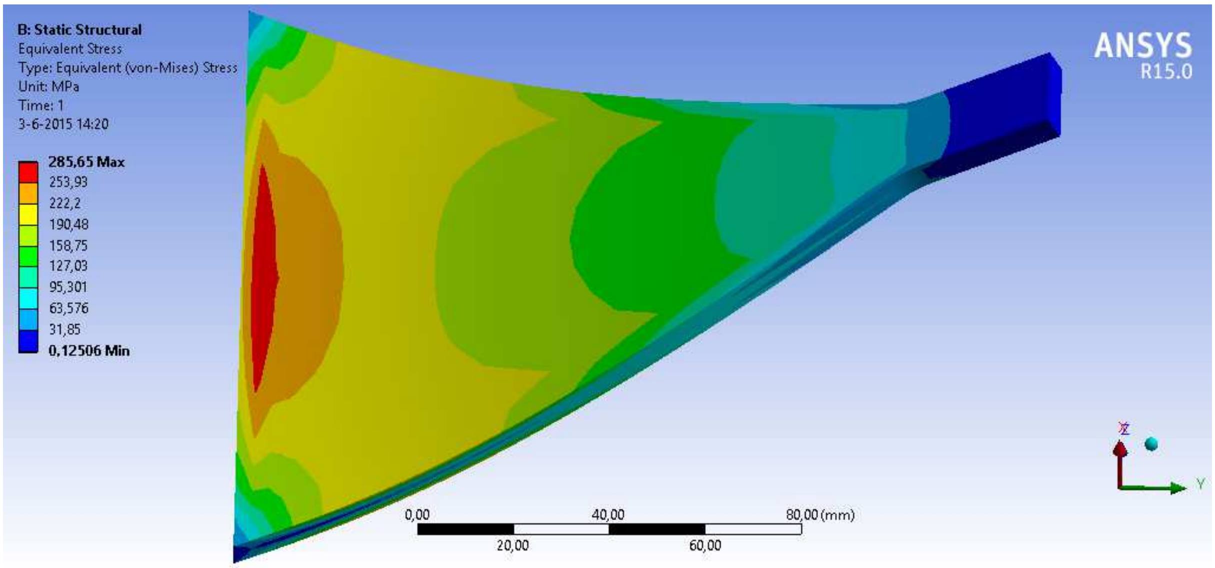

Figure 23: *ANSYS Workbench*: equivalent (von-Mises) stress

6 Testing method

The specimens are tested with different loading protocols.

6.1 Loading protocols

6.1.1 EN 15129

The loading protocol is EN 15129 (European Committee for Standardization (CEN), 2009). The amplitudes cycles will be increasing with regard to the design displacement Δ_D as following:

- 5 cycles of 25 % of Δ_D = 7,5 mm
- 5 cycles of 50 % of Δ_D = 15 mm
- 10 cycles of 100 % of Δ_D = 30 mm
- 1 cycle of $\gamma_b * \gamma_x * \Delta_D = 1{,}38 * \Delta_D$ = 41,4 mm
    - γ_b = partial factor for elastomeric isolators = 1,15
    - γ_x = magnification factor = 1,2

The force-displacement capacity is measured up to a displacement of $\gamma_b * \gamma_x * \Delta_D$ or the force up to $\gamma_b * \gamma_x * V_{Ebd}$. When one of those 2 values is reached, the test can be stopped.

6.1.2 ANSI/AISC 341-05

The loading protocol is ANSI/AISC 341-05 (American Institute of Steel Construction, 2005). The amplitudes cycles will be changing with regard to the yielding displacement Δ_y and the maximum displacement Δ_D as following:

- 2amplitude cycles of Δ_y= 6 mm
- 2amplitude cycles of $0{,}5*\Delta_D$= 15 mm
- 2amplitude cycles of Δ_D=30 mm
- 2 amplitude cycles of $1{,}5 *\Delta_D$= 45 mm
- 2 amplitude cycles of $2 *\Delta_D$ = 60 mm
- 4 amplitude cycles of $1{,}5 *\Delta_D$ 450 mm

After these cycles, the element will keep being tested at cycles of $1{,}5 *\Delta_D$ till it breaks.

6.1.3 Chosen loading protocols

The other elements will be tested at chosen protocols, the chosen protocols are:

- Amplitude cycles of $2 * \Delta_y = 12$ mm
- Amplitude cycles of $4 * \Delta_y = 24$ mm
- Amplitude cycles of $6 * \Delta_y = 36$ mm

6.2 *PCD 2K*

The loading machine runs on the software *PCD 2K*. The software controls the piston based on given displacement or given force. It is chosen to run the tests on given displacement with a triangular shaped curve in order to have a constant velocity. The loading protocols are programmed in the software taking into account following data:

- The number of cycles
- The amplitude
- The distance of one cycle
    - The distance of one cycle equals four times the amplitude.
- The velocity
    - The velocity equals 0,2 mm/s.
- Accuracy
    - There is a point given on the graph every 0,05 mm.

With this data the frequency can be calculated. Due to the software limits the frequency is accurate to 0,001 mm.

6.2.1 EN 15129

Table 1: Loading protocol EN 15129

Number of cycles	5	5	10	1
Amplitude [mm]	7,5	15	30	41,4
Distance (1 cycle) [mm]	30	60	120	165,6
Time (1 cycle) [s]	150	300	600	828
Frequency [Hz]	0,007	0,003	0,002	0,001

6.2.2 ANSI/AISC 341-05

Table 2: Loading protocol ANSI/AISC 341-05

Number of cycles	2	2	2	2	2	4
Amplitude [mm]	6	15	30	45	60	45
Distance (1 cycle) [mm]	24	60	120	180	240	180
Time (1 cycle) [s]	120	300	600	900	1200	900
Frequency [Hz]	0,008	0,003	0,002	0,001	0,001	0,001

6.2.3 Chosen loading protocols

With the chosen loading protocols there is no number of cycles taking into account, the tests continue until failure.

Table 3: Chosen loading protocols

Chosen loading protocol	1	2	3
Amplitude [mm]	12	24	36
Distance (1 cycle) [mm]	48	96	144
Time (1 cycle) [s]	240	480	720
Frequency [Hz]	0,004	0,002	0,001

7 Tests

7.1 General information

20 TADAS-specimens were made like designed except of one part. Design piece 5 (under the right part of the specimen) was made longer to be able to measure the displacement with transducers. Two transducers LVDT/150/01 are used for the tests, each on another side of the device. The range of these transducers is 150 mm and they are accurate to 0,01 mm. First a general view is given of the testing set-up:

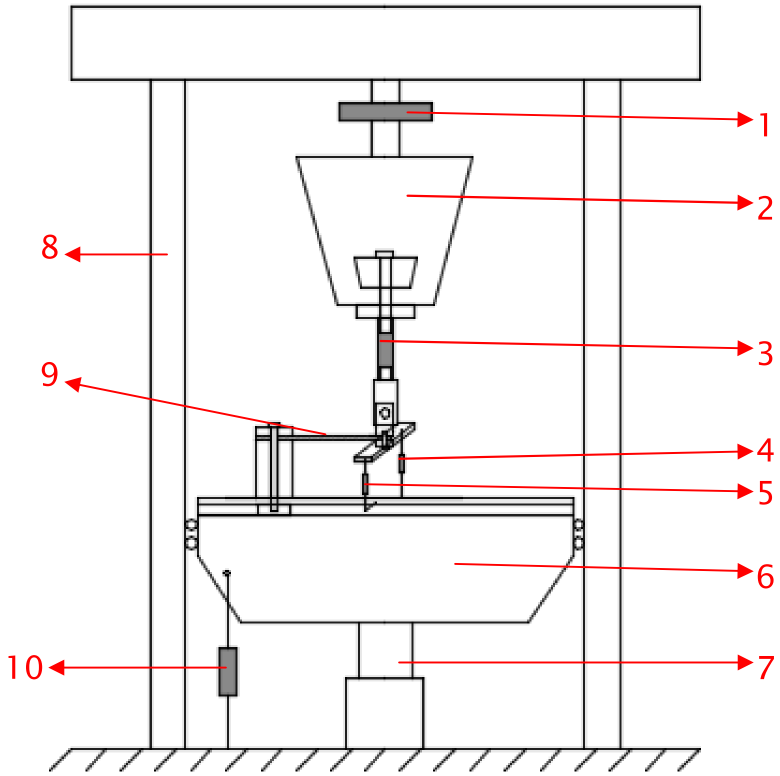

Figure 24: General view testing set-up

Explanation of the numbers on Figure 13:

1. Load cell of the machine
2. Fixed head of the machine
3. Load cell MODELO 630, nominal load of 2500 kg.
4. Displacement transducer LVDT/150/01 2
5. Displacement transducer LVDT/150/01 1
6. Mobile head of the machine
7. Piston of the machine

8. Glider
9. TADAS specimen
10. Displacement transducer of the machine

The displacement transducers LVDT/150/01 are fixed on design piece 5 in the following way:

Figure 25: Mounting of displacement transducers LVDT/150/01

The piston is located at the bottom of the machine and is controlled with the software *PCD 2K* (Servosis S.L.).

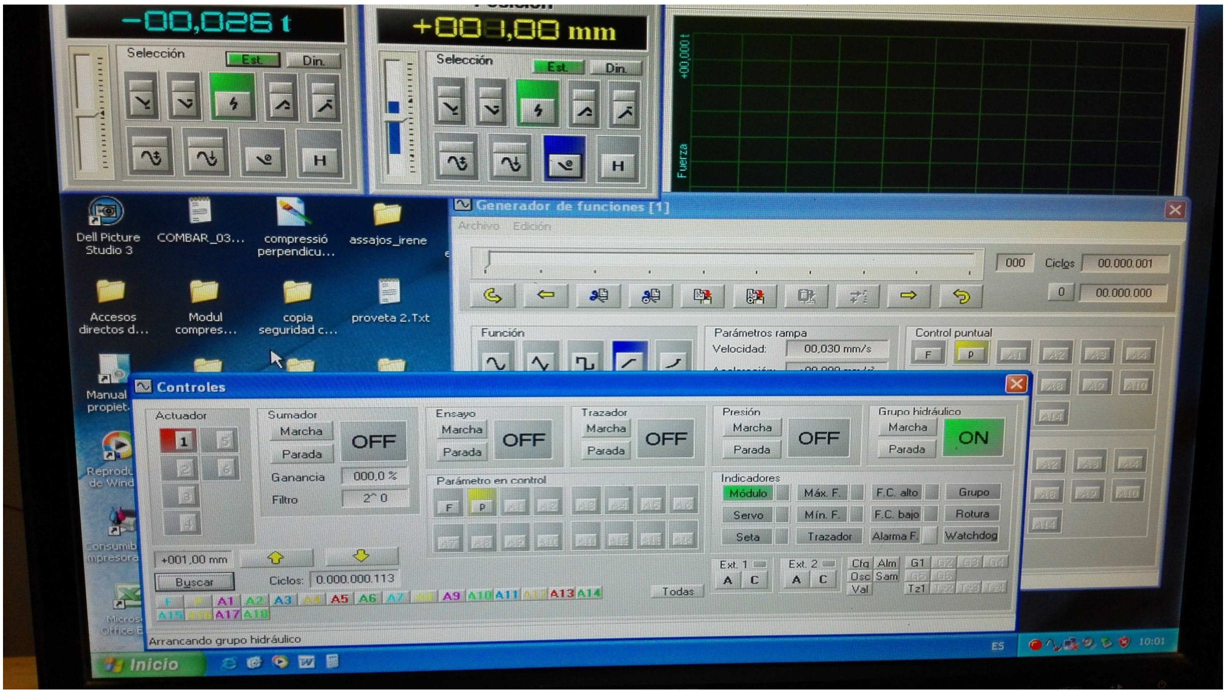

Figure 26: Overview software *PCD 2k*

The piston is controlled by the window 'Controles'. This window allows to:

- Turn the machine on/off.
- Move the piston upwards/downwards.
- Start/stop collecting data.
- Start/stop the loading protocol programmed in the window 'Generador de funciones [1]'.

The displacement of the piston and the force on the piston is measured and given in a force-displacement graph.

On a second computer the software *StrainSmart®* is run. *StrainSmart®* is a ready-to-use, Windows®-based software system for acquiring, reducing, presenting, and storing measurement data from strain gages, strain-gage-based transducers, thermocouples, temperature sensors, LVDT's, potentiometers, piezoelectric sensors and other commonly used transducers.

It is designed to function seamlessly with a variety of Micro-Measurements instrumentation hardware, including System 5000 *StrainSmart®* Data

Systems, which one is used for the tests (Micro-Measurements, 2011). There is 1 point measured every second.

Figure 27: Overview acquisition system

The test has been instrumented with 5 transducers, connected to the next channels of the acquisition system:

On the high card:

- #1: Load cell of the machine
- #2: Displacement transducer 1
- #4: Displacement transducer 2
- #11: Displacement transducer of the machine

- On the strain gage card:
  - #6: Load cell MODELO 630

The load cell of the machine has a range of 60 tons of compression to 60 tons of extraction while the load cell MODELO 630 has a range of 2,5 tons of compression to 2,5 tons of extraction.

7.2 Test 1

The first test is done with the chosen loading protocol 1. The amplitude is 12 mm and the frequency 0,004 Hz. The displacement of the TADAS-specimen is measured with two displacement transducers LVDT 150/01 and also with the displacement transducer of the machine. The average displacement measured by the displacement transducers LVDT 150/01 is compared with the displacement measured by the displacement transducer of the machine. The displacement is measured over the time and the first 250 useful seconds are displayed in following graph:

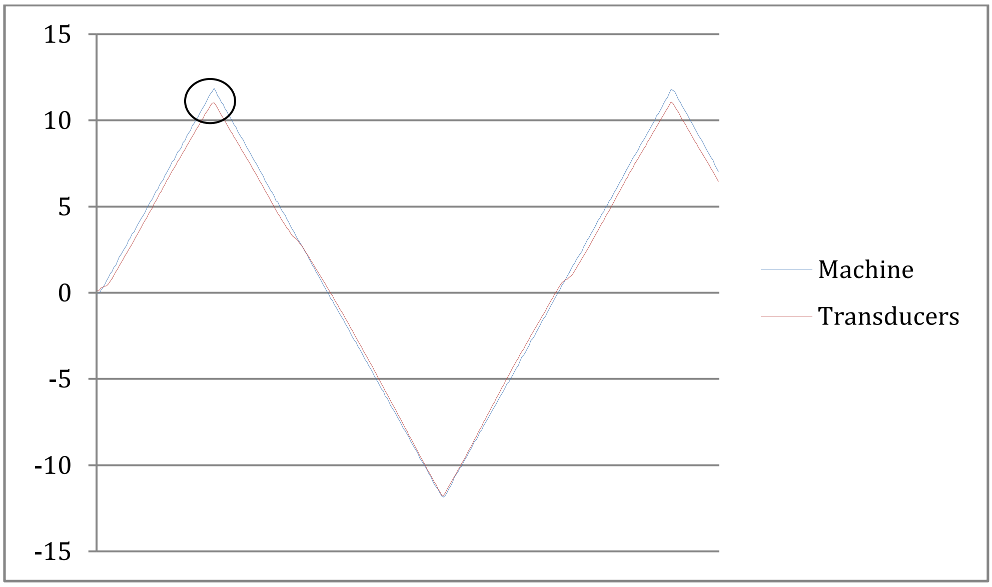

Figure 28: Displacement comparison graph

On the first top of the graph, the maximum values of the displacement are compared. These maximum values were measured at the same moment.

- Average displacement transducers LVDT/150/01: 11,01 mm
- Displacement transducer of the machine: 11,84 mm

The difference between both values is $\frac{11{,}84-11{,}01}{11{,}84} = 7\ \%$. This seems a lot, but the difference is only that big on the top of the curve.

Now the evolution of a force-displacement graph is compared.

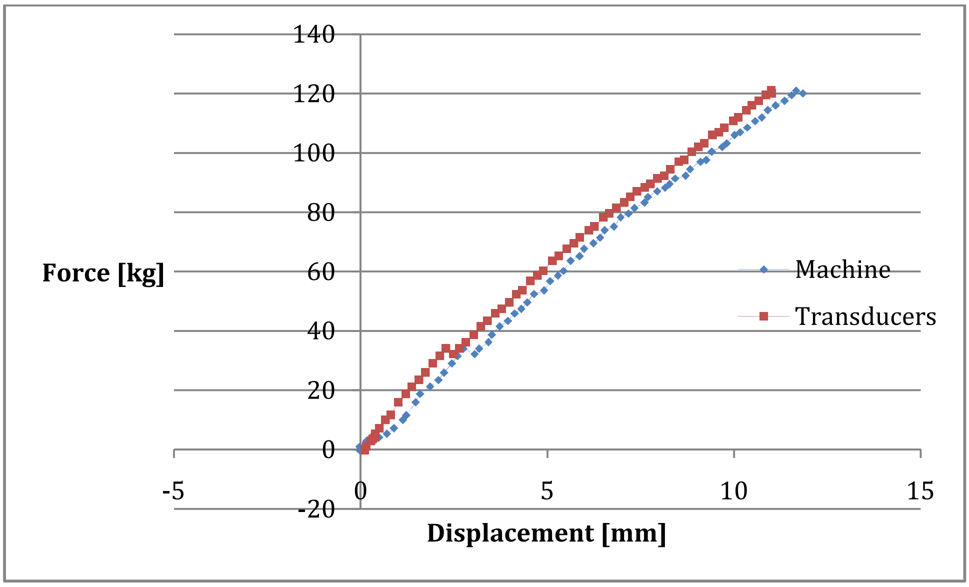

Figure 29: Force-displacement graph

This graph shows that for a given force, the displacement measured by the transducers is less than the displacement measured by the machine. This means that the deformation measured by the transducer of the machine is composed of the deformation in the test specimens plus the deformation of the other parts. The deformation of the machine would be neglected when large deformations of the specimen occurs (with large plastic components), but should be considered to determine the elastic stiffness of the specimen. So it would be better to use specific transducers to measure the relative deformation of the specimens.

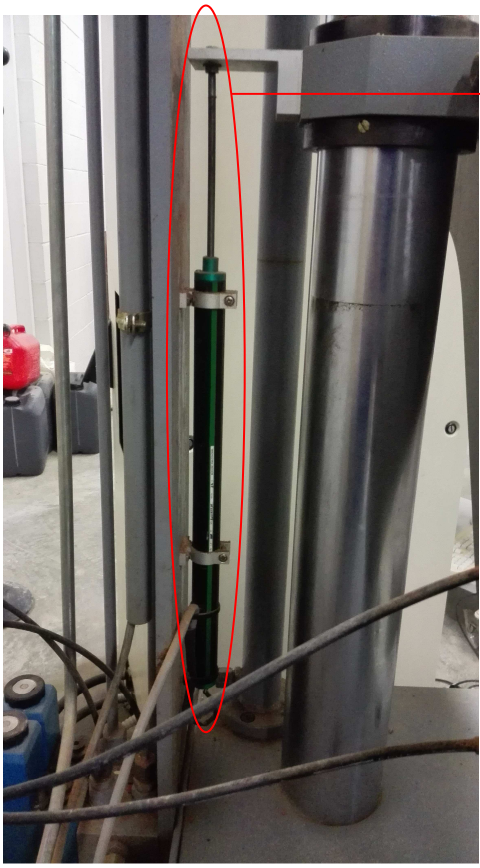

The displacement of the piston of the machine is measured by this appliance

Figure 30: Displacement transducer of the machine

From the results of test 1 it can be concluded that the displacement measured by the LVDT/150/01 transducers is not a big profit for the tests. The tests can be done with only taken into account the displacement of the piston measured by the machine.

7.3 Test 2

The second test is done with chosen protocol 2 and chosen protocol 3. The purpose of this test is to see how far the displacement can go with the testing set-up. The maximum displacement of the TADAS-device was 36 mm with chosen protocol 3. It was not advisable to submit the device to a larger displacement because the design only allowed a small horizontal displacement.

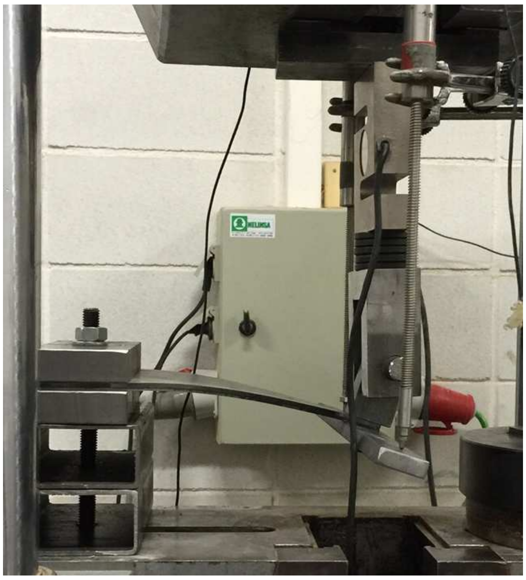

Figure 31: Image of test 2

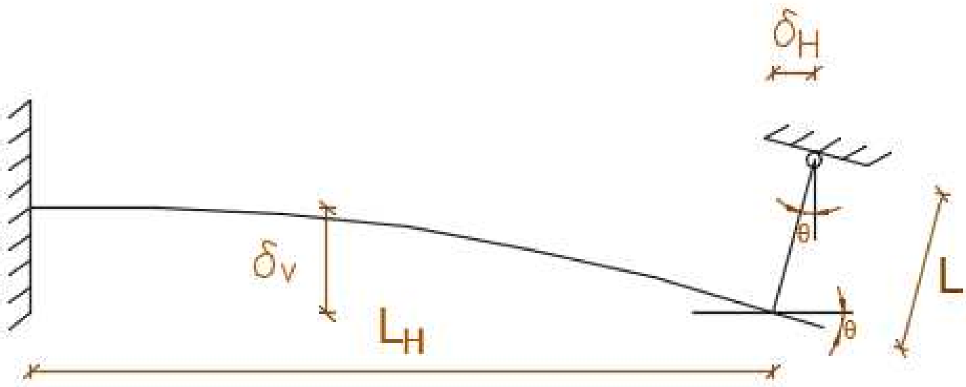

Figure 32: Simple representation of test 2

The system has just a capable solution for a δ_V and L has to satisfy it. This is applicable for all the δ_V points, so the design should be improved.

7.4 Test 3

For allowing a bigger horizontal displacement, the part that makes contact with the device had to be rounded. The lowest part of the set-up has been removed in order to achieve this. The idea behind this modification is given on the image below:

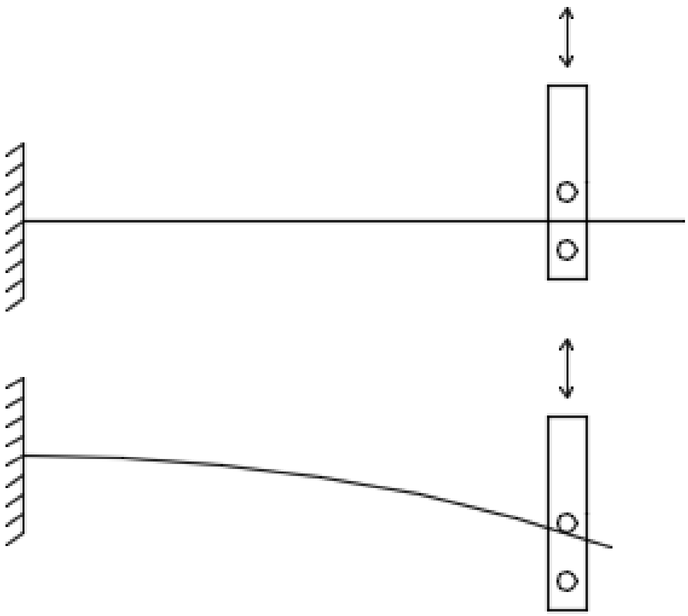

Figure 33: Simple representation of test 3

The specimen is located between 2 horizontal cylinders with a gap between them which is bigger than the thickness of the TADAS-device. In the given design there is only 1 cylinder, so the device could only be tested in one direction. If the test had succeeded, there could be made a new hole in each side of the piece in order to put a second cylinder through design piece 3 and be able to test in both the directions.

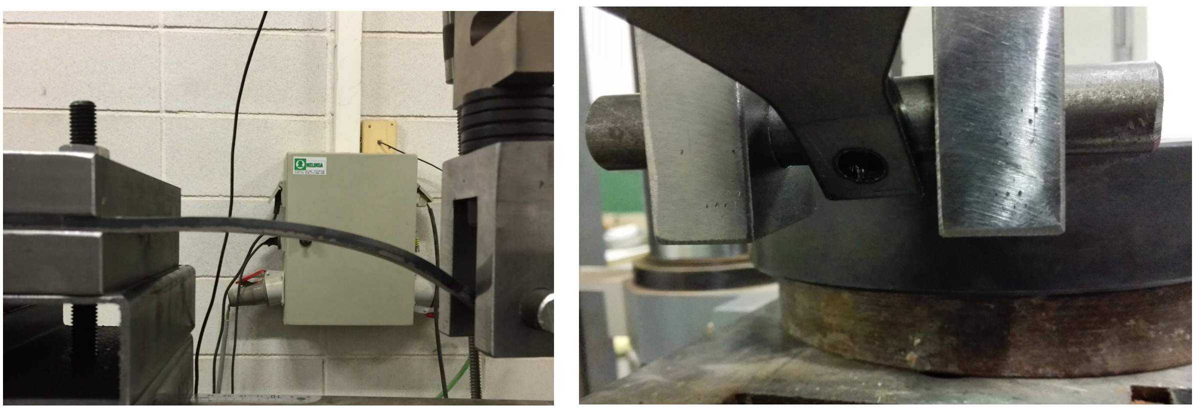

Figure 3: Image of test 3

With this test a deformation of approximately 50 mm was achieved. This modification had 2 problems:

- The vertical displacement causes a horizontal displacement. When this horizontal displacement becomes too high, the device gets out of the testing emplacement.
- The resulting force is diagonal oriented which causes on his turn 2 other problems:
    - The resulting force consists of a horizontal and a vertical force but only the vertical force can be measured by the load cell.
    - The horizontal force causes a bending moment in the load cell. When this moment becomes too high, the load cell could get damaged.

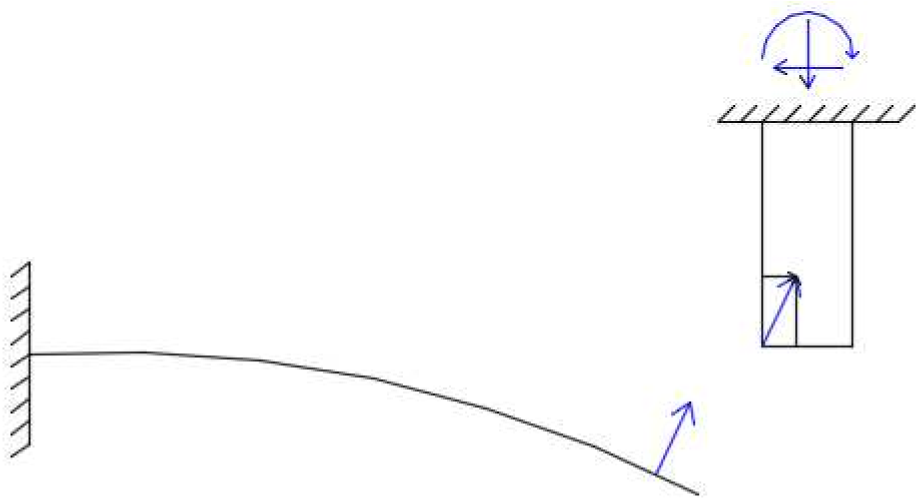

Figure 34: Schematic view bending moment in load cell MODELO 630

8 Proposal for future design

A new proposal for future design is made. At the end of the TADAS-device there is a cylinder which will be attached in a case in order to allow free horizontal displacement.

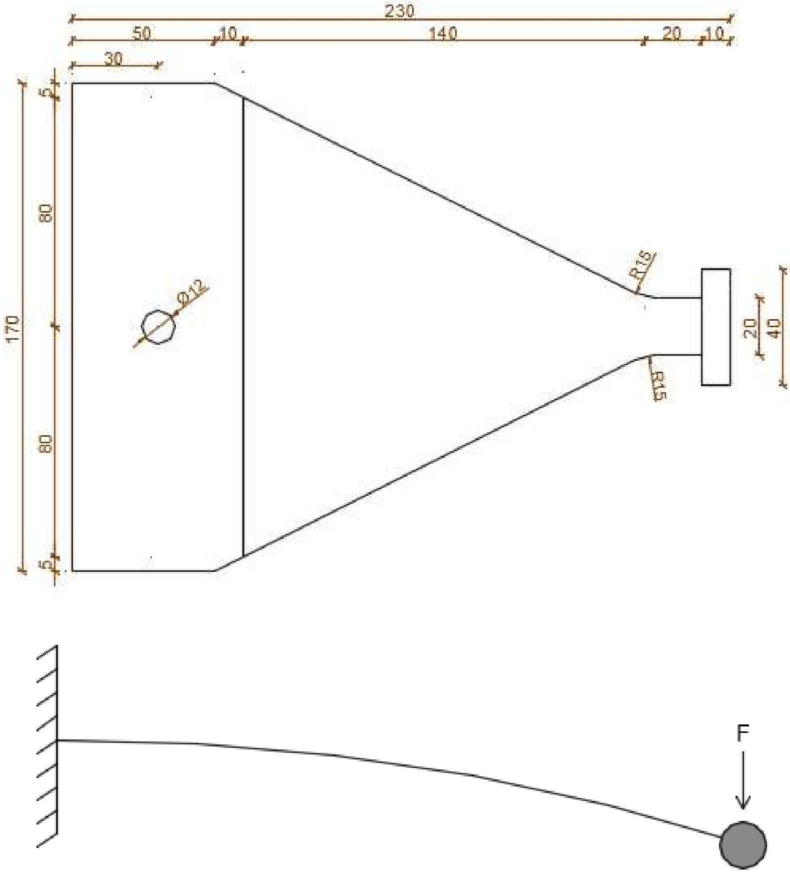

Figure 35: Proposal geometry TADAS-specimen for future design

The lowest part of the testing mechanism could be made as following:

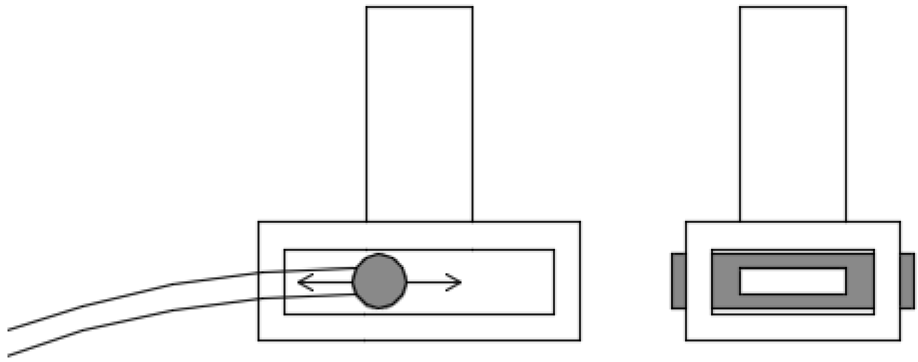

Figure 36: Proposal of future design: lowest part of the testing set-up

The device is free to move in the horizontal direction to a certain displacement. This has as result that the only forces which engage the testing mechanism are vertical. In this way the load cell can't be damaged and measures more accurate. The system to install into a building could have this shape:

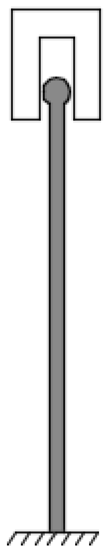

Figure 37: Proposal of future design: Installation method in buildings

This drawing is based on an image from a paper about the use of dual systems in TADAS dampers to improve the seismic behavior of buildings in different levels.

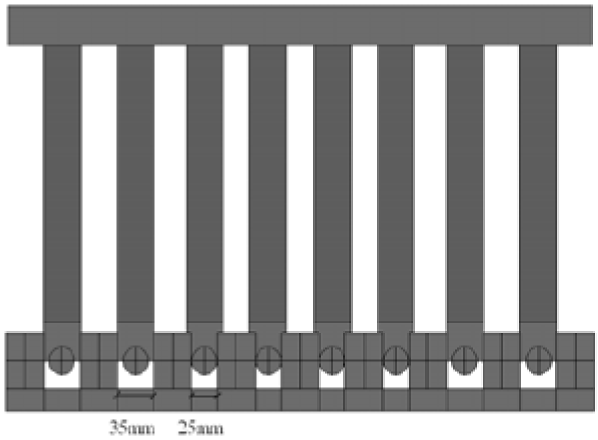

Figure 38: Modified-TADAS Configuration (Dareini & Hashemi, 2011)

9 Conclusions

- It has been demonstrated the specimen is too small to satisfy the interstory drift corresponding to 3 m high stories.
- It has been demonstrated the first design was not correct because it didn't allow free rotation and it produced an undesired bending moment in the load cell.
- From the tests it has been seen that the load-deformation responses can be provided by the machine transducer and an additional small load cell with a nominal load of 2500 kg.
- A final test design is proposed, much similar to the real working conditions of the TADAS in buildings.

10 Acknowledgement

I would like to thank some people that have been helping me to finish my master thesis. Especially my EPS Advisor Xavier Cahis for assisting me during my whole thesis. I also want to thank Sergi Saus and Jordi Vicens from the mechanical lab for making the pieces of the testing set-up. Further I also want to thank Pedro Bellheví to help me with the tests.

11 Overview of the used tables and figures

11.1 Tables

11.2 Figures

12 Bibliography

American Institute of Steel Construction. (2005). *ANSI/AISC 341s1-05 Seismic Provisions of Structural Steel Buildings.* Chicago, Illunois.

ANSYS. (2015, June 3). Retrieved June 3, 2015, from Website of ANSYS: http://www.ansys.com/Resource+Library/Webinars/Using+Remote+Boundary+Conditions+in+ANSYS+Mechanical

Bureau voor Normalisatie. (2005). *Eurocode 3: Ontwerp en berekening van staalconstructies - Deel 1-8: Algemene regels - Ontwerp en berekening van verbindingen (+AC:2005 +AC:2009) .* Brussel.

Dareini, H. S., & Hashemi, B. H. (2011). Use of Dual Systems in Tadas Dampers to Improve Seismic Behavior of Buildings in Different Levels. *Procedia Engineering 14* (pp. 2788-2795). Elsevier Ltd.

European Committee for Standardization (CEN). (2001). *EN 10002-1 Metallic materials - Tensile testing - Part 1: Method of test at ambient temperature.* Brussels.

European Committee for Standardization (CEN). (2009). *Final Draft FprEN 15129 Anti-seismic devices.* Brussels.

Fajdiga, G., & Sraml, L. (2009). Fatigue crack initiation and propagation uncer cyclic contact loading. *Engineering Fracture Mechanics 76* , 1320-1335.

Gallego, A., Benavent-Climent, A., & Romo-Melo, L. (2015). Piezoelectric sensing and non-parametric statistical signal processing for health monitoring of hysteretic dampers used in seismic-resistant structures. *Mechanical Systems and Signal Processing 60-61* , 90-105.

Ganesh, P., Sundar, R., Kumar, H., Kaul, R., Ranganathan, K., Hedaoo, P., et al. (2014). Studies on fatigue life enhancement of pre-fatigued spring steel specimens using laser shock peening. *Materials and Design 54* , 734-741.

Inoue, K., & Kuwahara, S. (1998). optimum strength ratio of hysteretic damper. *Earthquake engineering and structural dynamics* , 577-588.

Mahmoudi, M., & Abdi, M. G. (2011). Evaluating response modification factors of TADAS frames. *Journal of Constructional Steel Research* , 162-720.

Micro-Measurements. (2011, May 4). Retrieved June 9, 2015, from StrainSmart® Data Acquisition System: http://www.vishaypg.com/docs/11268/strainsm.pdf

Nakashima, M., Saburi, K., & Tsuji, B. (1996). Energy input and dissipation behaviour of structures with hysteretic dampers. *Earthquake engineering and structural dynamics* , 483-496.

Open Steel Joists. (n.d.). *Buckling Restrained Brace*. Retrieved June 12, 2015, from http://www.open-joist.com/english/product3_5.asp

Piedrafita, D., Cahis, X., Simon, E., & Comas, J. (2015). A new perforated core buckling restrained brace. *Engineering structures 85* , 118-126.

Servosis S.L. (n.d.). *Software*. Retrieved Juni 11, 2015, from Servosis: http://www.servosis.com/productos.html

Zhou, H., Wang, Y., Yang, L., & Shi, Y. (2014). Seismic low-cycle fatigue evaluation of welded beam-to-column connections in steel moment frames through global-local analysis. *Internation Journal of Fatigue 64* , 97-113.

Annex A : Glossary of symbols

Table 4: Glossary of symbols

Symbol	Unit	Designation
f_{ub}	Mpa	Ultimate tensile strength of the bolt
f_{yb}	Mpa	Ultimate yielding strength of the bolt
t	mm	Thickness specimen
k	/	Coefficient of proportionality
y_{max}	mm	Distance from centroidal axis to the end of the section
A_s	mm^2	Stress section of the bolt
B	mm	Width
E	Mpa	Young's modulus
F_b	N	Required bolt tensile strength
$F_{t,Rd}$	N	Design value of the tensile strength per bolt
I	mm^4	Moment of inertia
L	mm	Length
L_0	mm	Original gauge length
L_c	mm	Parallel length

M	Nmm	Moment
S_0	mm^2	Original cross-sectional area of the parallel length
V_{Ebd}	N	Design shear force
γ_b	/	Partial factor for elastomeric isolators
γ_x	/	Magnification factor
δ_d	mm	Design displacement
δ_y	mm	Yielding displacement
ϵ_y	/	Yielding strain
θ	rad	Angle
σ_y	Mpa	Yielding stress
Δ_d	mm	Design displacement
Δ_y	mm	Yielding displacement

Annex B : Geometry of the pieces of the testing set-up

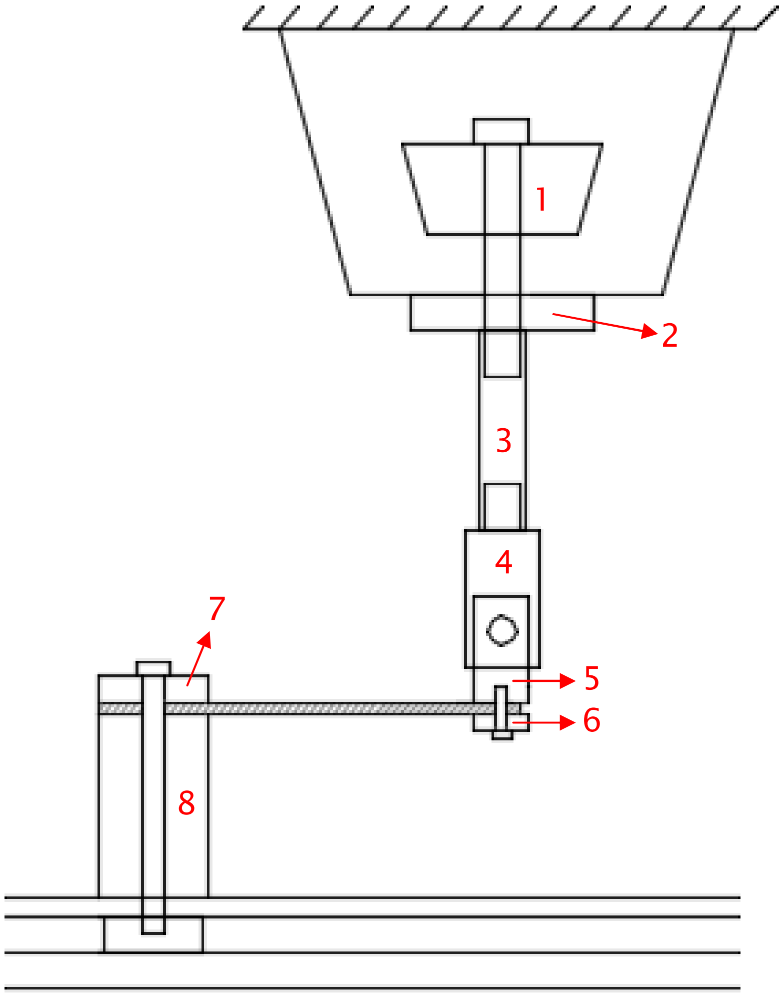

Figure 39: Summary of the set-up pieces

Explanation of the numbers on Figure 13

1. Available piece 1
2. Design piece 1
3. Load cell MODELO 630
4. Design piece 2
5. Design piece 3
6. Design piece 4
7. Design piece 5
8. Design piece 6

Available Piece 1:

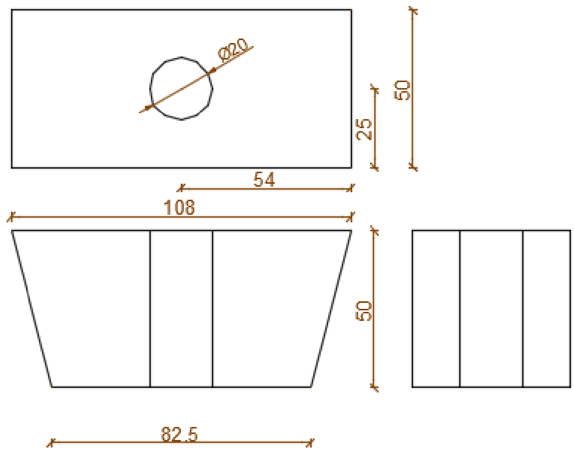

Figure 40: Available piece 1

Design piece 1:

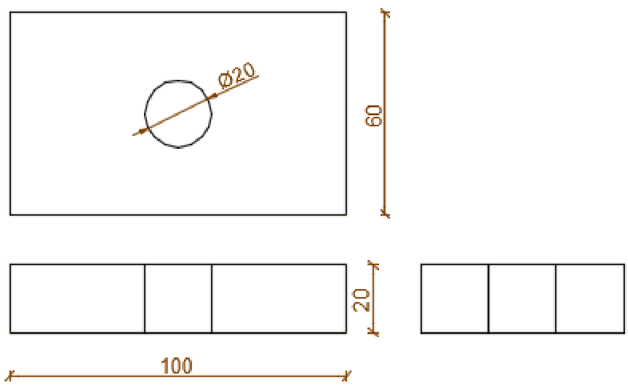

Figure 41: Design piece 1

Load cell: Modelo 630

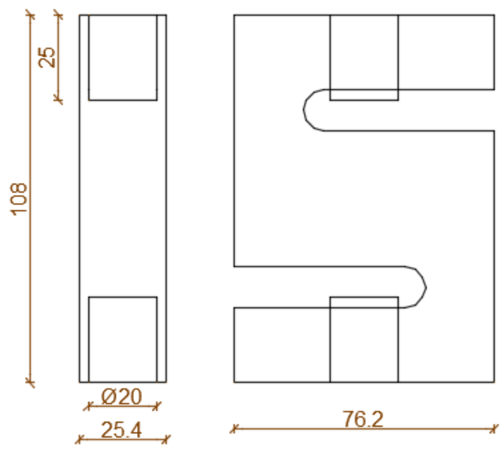

Figure 42: Load cell MODELO 630

Design piece 2:

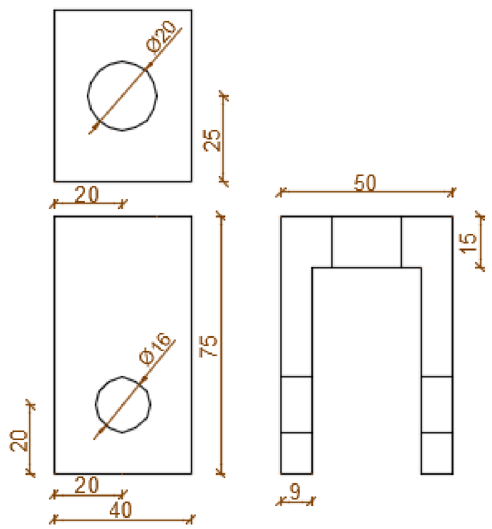

Figure 43: Design piece 2

Design piece 3:

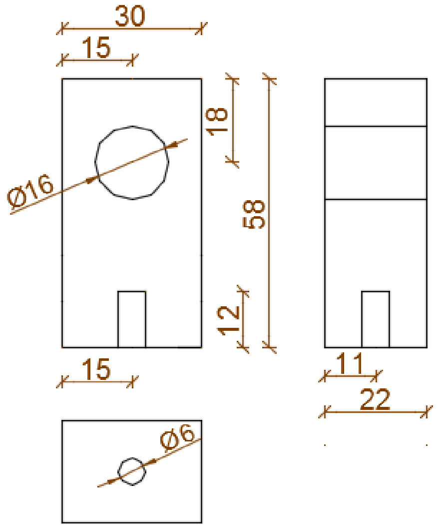

Figure 44: Design piece 3

Design piece 4:

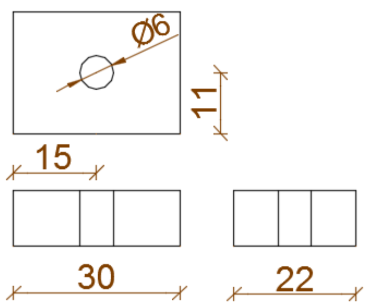

Figure 45: Design piece 4

Design piece 5 (2x):

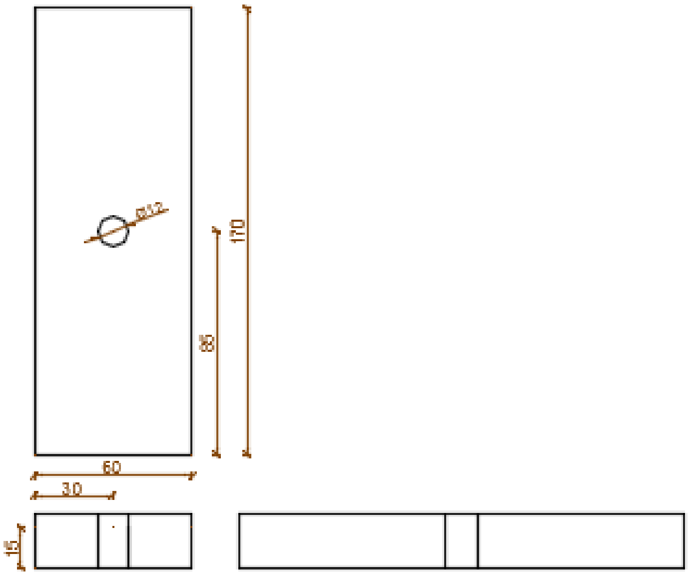

Figure 46: Design piece 5

Design piece 6 (2x):

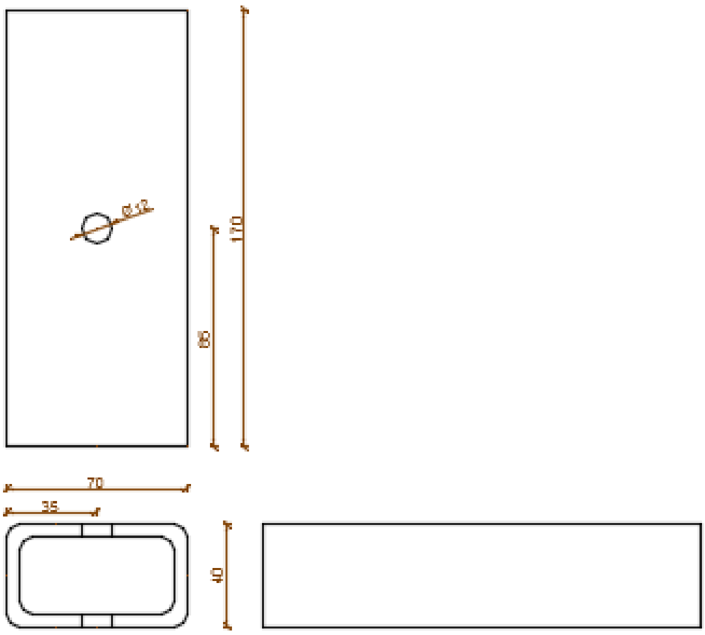

Figure 47: Design piece 6

Annex C :Technical specifications of load cell MODELO 630

UTILCELL CELULAS DE CARGA - LOAD CELLS

MODELO 630

50kg...2500kg

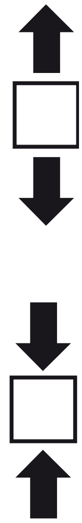

- Célula de carga de tracción/compresión
- 3000 divisiones O.I.M.L. R60 clase C
- Soporte elástico de acero aleado
- Protección IP 67 (EN 60529)
- Tratamiento anticorrosión de níquel duro
- Aplicaciones:
  - Tanques, Tolvas y Cintas pesadoras suspendidas de estructuras
  - Centrales de asfalto y hormigón
  - Medida de fuerza en maquinaria de ensayo
  - Pesaje aéreo

- Tension/compression load cell
- 3000 divisions O.I.M.L. R60 class C
- Measuring element from Steel alloy
- Protected IP 67 (EN 60529)
- Protected against corrosion by nickel-plated treatment
- Applications:
  - Suspended weighing in Tanks, Hoppers and Belt Conveyor Scales
  - Asphalt and Concrete Plants
  - Force measurement in Test Equipment
  - Crane scales

Modelo Model	Carga nominal Nominal capacity Ln	Clase de precisión Accuracy class n. OIML	División mínima Minimum division vmin	Carga de servicio Service load 150% Ln	Carga límite Safe load 300% Ln
630 50 kg	50 kg	3000	5 g	75 kg	150 kg
630 100 kg	100 kg	3000	10 g	150 kg	300 kg
630 250 kg	250 kg	3000	25 g	375 kg	750 kg
630 500 kg	500 kg	3000	50 g	750 kg	1500 kg
630 1000 kg	1000 kg	3000	100 g	1500 kg	3000 kg
630 2500 kg	2500 kg	3000	250 g	3750 kg	7500 kg

MODELO 630

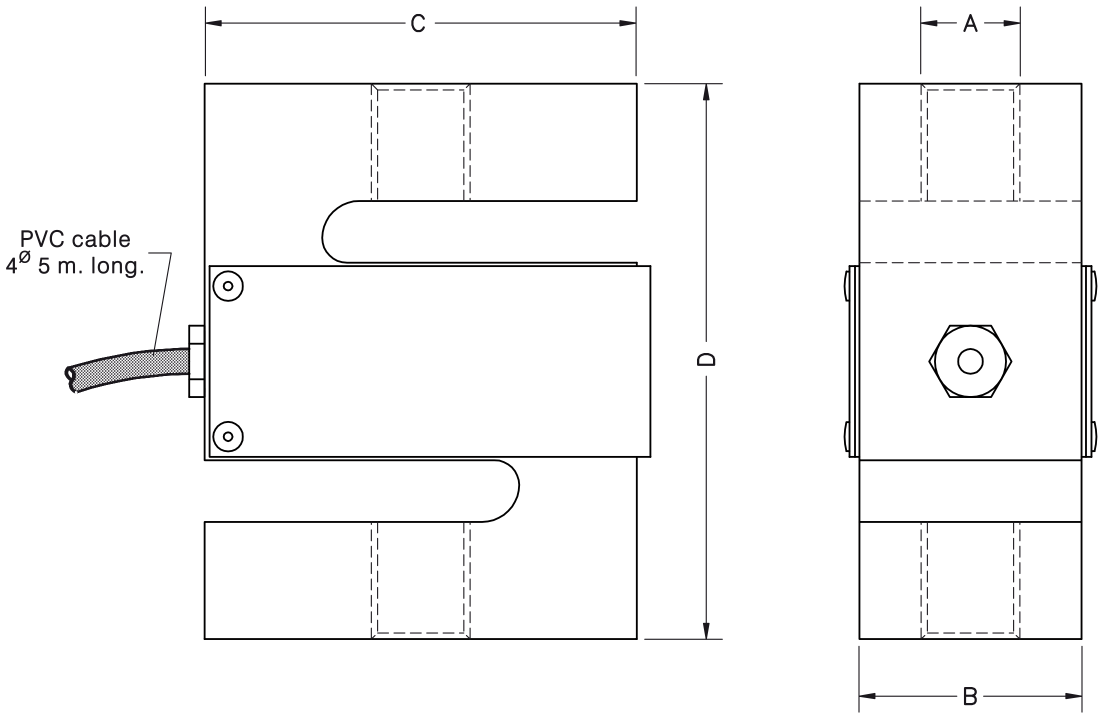

Carga nominal Nominal load	A	B	C	D	Peso transporte Transport weight
50-100 kg	M8x1.25	15	50.8	63.5	0.4 kg
250-500-1000 kg	M12x1.25	19	50.8	76.2	0.6 kg
2500 kg	M20x1.5	25.4	76.2	108	1.3 kg

Dimensiones en mm. *Dimensions in mm.*

ESPECIFICACIONES			SPECIFICATIONS
Cargas nominales (Ln)	50-100-250 500-1000-2500	kg	Nominal capacities (Ln)
Clase de precisión	3000	n. OIML	Accuracy class
Carga mínima Carga de servicio Cargas límite	0 150 300	%Ln %Ln %Ln	Minimum dead load Service load Safe load limit
Error combinado Error repetibilidad	< ±0.017 < ±0.015	%Sn %Sn	Total error Repeatability error
Efecto de la temperatura: en el cero en la sensibilidad	 < ±0.01 < ±0.006	 %Sn/5°K %Sn/5°K	Temperature effect: on zero on sensitivity
Error de fluencia (30 minutos)	< ±0.016	%Sn	Creep error (30 minutes)
Compensación de temperatura Límites de temperatura	-10...+40 -30...+70	°C °C	Temperature compensation Temperature limits
Sensibilidad nominal (Sn) Tensión de alimentación nominal Tensión de alimentación máxima Resistencia de entrada Resistencia de salida Desequilibrio inicial Resistencia de aislamiento	2 ±0.1% 10 15 400 ±20 350 ±3 < ±2 > 5000	mV/V V V Ω Ω %Sn MΩ	Nominal sensitivity (Sn) Nominal input voltage Maximum input voltage Input impedance Output impedance No load output Insulation resistance
Deformación máxima (a Ln)	0.3-0.5	mm	Maximum deflection (at Ln)

CONEXION ELECTRICA
ELECTRICAL CONNECTION:

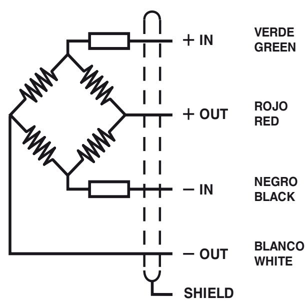

«CONVENIO SIGNOS SALIDA PARA TRACCIÓN»

«OUTPUT SIGNS FOR TENSION APPLICATION»

1423

UTILCELL
CELULAS DE CARGA - LOAD CELLS

ACC. TE8x1.25
ACC. TE12x1.25
ACC. TE20x1.5

ACCESORIO TRACCION PARA MOD. 630
TENSION ACCESSORY FOR MODEL 630

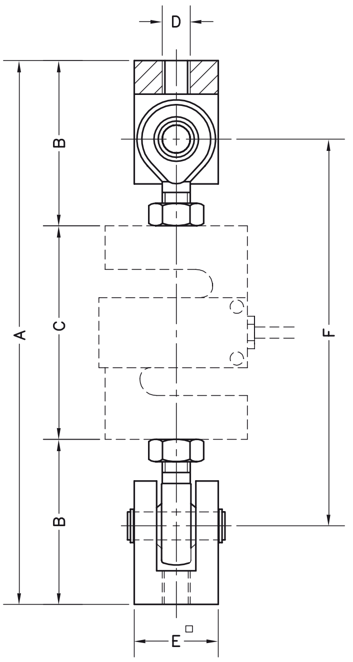

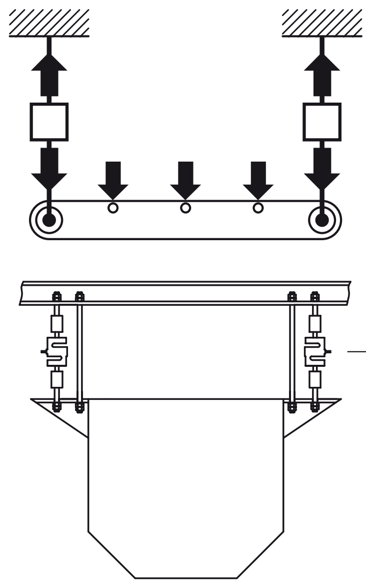

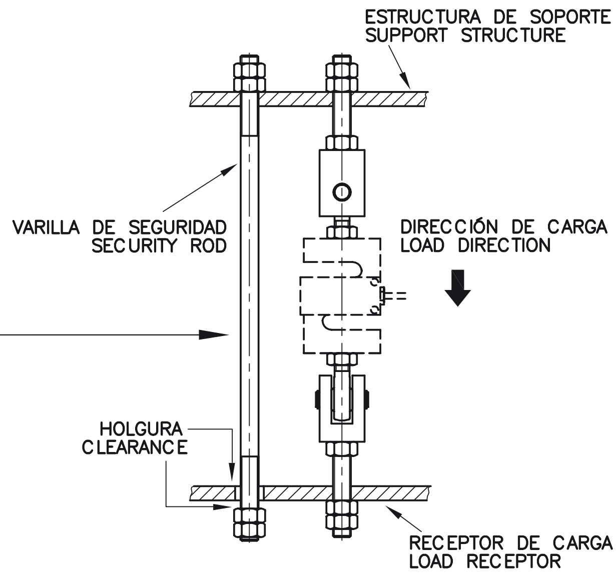

Accesorio Accessory	Carga nominal Nominal load	A	B	C	D	E□	F	Carga límite Ultimate load	Peso transporte Transport weight	Material
TE8x1.25	50-100 kg	181	58.8	63.5	M8x1.25	25	125	400 kg	0.6 kg	Acero cincado Steel zinc-plated
TE12x1.25	250-500-1000 kg	242.2	83	76.2	M12x1.75	35	154.2	2580 kg	1.4 kg	
TE20x1.5	2500 kg	340	116	108	M20x2.5	50	212	5050 kg	4.5 kg	

Dimensiones en mm. *Dimensions in mm.*

1423

UTILCELL
CELULAS DE CARGA - LOAD CELLS

ACC. RO8x1.25
ACC. RO12x1.25
ACC. RO20x1.5

ROTULAS PARA EL MODELO 630
ROD ENDS FOR MODEL 630

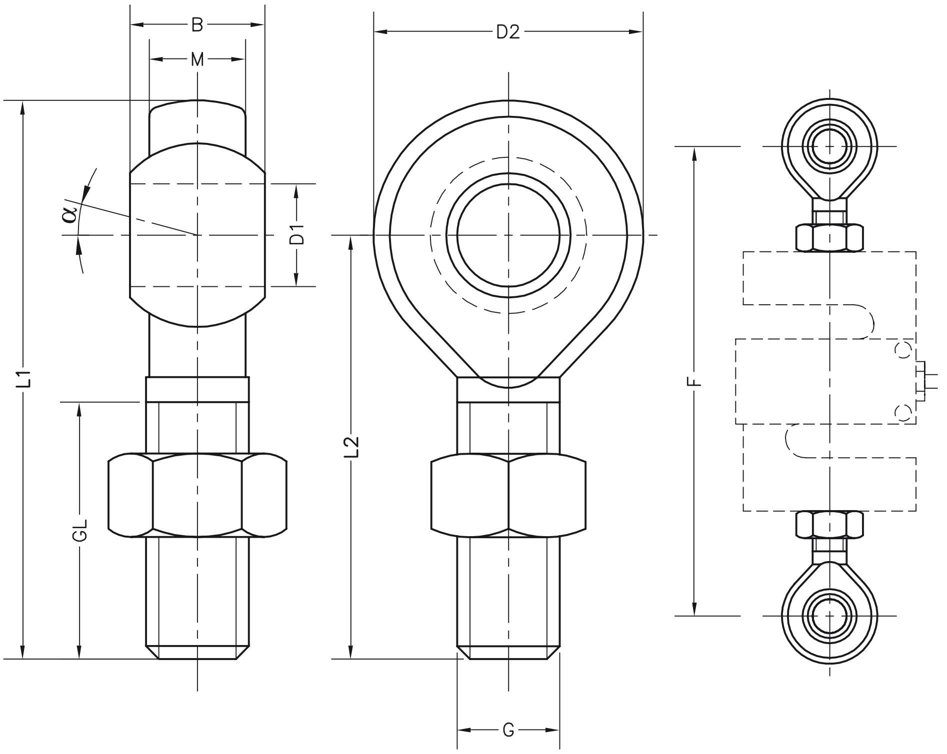

- **Material: Acero cincado**
- **Cada accesorio RO contiene un juego de: 2 rótulas y 2 tuercas**

- **Material: Steel zinc-plated**
- **Each accessory RO includes a set of: 2 rod ends and 2 nuts**

Dimensiones Accesorios RO/ *RO* Accessories Dimensions

Accesorio Accesory	Capacidad/ Capacity (kg)	D2	B	M	D1	L1	L2	GL	G	α	F	Peso transp. Trans. weight
RO8x1.25	50-1000	24	12	9	Ø8	54	42	25	M8x1.25	13°	125	0.2 kg
RO12x1.25	250-500-1000	32	16	12	Ø12	70	54	33	M12x1.25	13°	154.2	0.2 kg
RO20x1.5	2500	50	25	18	Ø20	103	78	47	M20x1.5	15°	212	0.8 kg

Dimensiones en mm. *Dimensions in mm.*